

## 6. FIRST PALYNOLOGICAL RESULTS FROM SITE 658 AT 21°N OFF NORTHWEST AFRICA: POLLEN AS CLIMATE INDICATORS<sup>1</sup>

Lydie M. Dupont,<sup>2</sup> Hans-Jürgen Beug,<sup>2</sup> Hartmut Stalling,<sup>2</sup> and Ralf Tiedemann<sup>3</sup>

### ABSTRACT

Ocean Drilling Program Site 658 at 21°N off northwest Africa has a high sedimentation rate and a high concentration of pollen grains and is thus very suitable for detailed pollen analysis.

The time scale for the upper 100 m (the last 670 k.y.) of Site 658 is based on biostratigraphic data and isotope stratigraphy. The pollen record has been divided into 34 zones. These are classified into 7 zone types covering a range from very arid to rather humid conditions.

The sequence shows a long-term climatic decline: strong glacial stages were found only after 480 k.y. and strong interglacial stages only before 280 k.y. The Site 658 record correlates well with a terrestrial sequence from northern Greece, although both records differ in their response to global climatic change.

Spectral analysis shows a 100- and a 42-k.y. period in the curves of pollen brought in by the northwest trade winds and only a 42-k.y. period in the curves of pollen mostly transported by the African Easterly Jet. A 31-k.y. period is found in the curves for *Ephedra* and Chenopodiaceae-Amaranthaceae. In addition, *Ephedra* shows a 54-k.y. period.

### INTRODUCTION

This paper presents the first results of palynological investigations of sediments from Ocean Drilling Program (ODP) Site 658 with some remarks on Site 661. Palynological work on marine sediments of the last 130 k.y. has been done by Caratini et al. (1979) on material of the ORGON III expedition west of Cap Blanc and from the Kayar Canyon. Rossignol-Strick and Duzer (1979) studied three meteor cores northwest of Dakar covering the last 22.5 k.y. These studies recognized the importance of wind transport of pollen into the Atlantic. A grouping based on the geographical origin of the pollen taxa was made. Agwu and Beug (1982) further explored the possibility of marine palynological work in meteor cores between 33°N and 7°N off the West African coast. Melia (1984), using *Atlantis II* material, related the pollen and aerosols demonstrating the influence of the prevailing wind direction off the coast of northwest Africa.

A study of more than 100 surface and core-top samples from the marine sediments west of Africa between 34°N and 6°N (Hooghiemstra et al., 1986) confirmed that in this area, pollen transport by wind is much more efficient than transport by water (ocean currents). Furthermore, several pollen types were found to be indicators of transport by individual wind systems, mainly the northeast trade winds and the African Easterly Jet (AEJ).

These results, obtained from the modern situation, were subsequently used as a basis for interpreting older marine cores mostly situated on the trajectory of the northeast trade winds and the AEJ. Hooghiemstra (1988a) studied meteor core M 16017-2 located near the site of Hole 658 off Cap Blanc at 21°N. The pollen sequence in this core covers the interval from 20 to 5 k.y. (isotope stages 2 and 1). Site 658 and core M

16017-2 are both situated on the trajectories of the trade winds and the AEJ.

The results of Hooghiemstra (1988a) confirmed those of Sarnthein and Koopmann (1980) and Sarnthein et al. (1982): the AEJ remained stable in its position despite glacial/interglacial climatic fluctuations. Therefore, the pollen assemblage transported to the core site at 21°N from eastern source areas depends on the type of vegetation in the source area of the AEJ. In more arid periods, the AEJ dust load contains more Chenopodiaceae-Amaranthaceae pollen. In humid periods, grass pollen from the Savanna and Sahel Zones will be blown in high quantities westward to the Atlantic Ocean because those zones shifted northward during periods more humid than today.

The northeast trade winds appear to have remained in their present position through the different isotope stages but to have changed in strength. A comparison between terrestrial palynological sequences from Spain and Morocco with marine cores revealed that strong northeast trade winds in glacial periods caused an increased pollen influx, while in interglacial periods the pollen transport by the weaker trade winds was diminished (Hooghiemstra, 1989).

Since Site 658 is located in the trajectories of two wind systems, each of them contribute to the pollen influx of Poaceae (grasses) and Chenopodiaceae-Amaranthaceae. River runoff, as indicated by *Rhizophora* pollen, has been found to occur just after the end of the dry period from 20 to 14 k.y. (Rossignol-Strick and Duzer, 1979; Hooghiemstra, 1988b).

The ultimate aim of palynological investigations of ODP sites is to extend pollen studies to the bottom of Site 658 at an age of about 3.5 Ma. The present report deals mainly with the first 100 m of Site 658 covering isotope stages 1 to 17 (Holocene to middle Pleistocene). It includes some preliminary remarks on Site 661.

This paper reports on the character of the different isotope stages with respect to vegetation, climate, wind transport, and pollen productivity (influx). We show initial results of spectral analysis. A quantitative evaluation of the importance of the individual wind systems is given by Dupont (1989).

### MATERIAL AND METHODS

Site 658 is situated at 20°44.95'N and 18°34.85'W at a water depth of 2263 m on the continental slope 160 km west of Cap Blanc. Three

<sup>1</sup> Ruddiman, W., Sarnthein, M., et al., 1989. Proc. ODP, Sci. Results, 108: College Station, TX (Ocean Drilling Program).

<sup>2</sup> Institut für Palynologie und Quartärwissenschaften, Universität Göttingen, Wilhelm-Weber-Strasse 2, 3400 Göttingen, Federal Republic of Germany.

<sup>3</sup> Geologisch-Paläontologisches Institut, Universität Kiel, Olshausenstrasse 40, D-2300 Kiel, Federal Republic of Germany.

holes were cored: 658A, 658B, and 658C. The oldest sediments, with an estimated age of 3.5–3.8 Ma, were reached in Hole 658A at a sub-bottom depth of 300 m (Ruddiman, Sarnthein, et al., 1988). Pollen samples were taken from cores of Hole 658A and from the upper nine cores of Hole 658B. Correlation of Holes 658A and 658B was established by means of magnetic susceptibility, and the composite depths of both sections were computed (Ruddiman, Sarnthein, et al., 1988; Sarnthein and Tiedemann, this vol.).

Site 661 is situated at 9°26.81'N and 19°23.17'W at a water depth of 4012 m on a plateau east of Kane Gap near the Sierra Leone Rise. Two holes were cored, and pollen samples were taken from the upper 12 cores of Hole 661A. The oldest pollen sample comes from a sub-bottom depth of 105 m with an estimated age of 66 Ma (Ruddiman, Sarnthein, et al., 1988).

Pollen samples from Site 661 are about 25 cm<sup>3</sup>, although sample volumes of about 15 cm<sup>3</sup> were sufficient for Site 658. The volume of these samples was determined by water displacement, and the wet samples were then split over a 250-μm sieve. The coarse fraction was used for oxygen isotope measurements by R. Tiedemann to improve the resolution of the oxygen isotope curve to about 2600 yr.

The fraction smaller than 250 μm was decalcified with HCl and treated with warm KOH. *Lycopodium* marker tablets were added together with the HCl. Sand and clay were removed with HF, the sample was acetolyzed, and finally particles smaller than 10 μm were removed by ultrasonic sieving. Pollen grains were mounted in glycerin jelly. The slides were analyzed by L. Dupont and H. Stalling. The total number of counted pollen, added and counted *Lycopodium* marker spores, and a sample volume of Site 658 are given in Appendix B. In identifying pollen grains, we used the reference collection at the Institute for Palynology (Göttingen) and the literature listed by Agwu and Beug (1982). In addition, we used Ybert (1979) and Bonnefille and Riollet (1980).

The pollen data of Site 658 are presented as influx values and as percentages of the total pollen counted. The influx values were computed from the concentration values and the sedimentation rates. The concentration values were determined by reference to the known number of *Lycopodium* markers and expressed per cm<sup>3</sup>. Both influx values and percentages are plotted against a time scale derived from Sarnthein and Tiedemann (this vol.). In the summary diagram, all pollen types recognized are clustered into six groups (see Appendix A), representing different pollen source areas.

Spectral analysis was carried out with the Fortran programs CROSPEC and SPECTDF on a microcomputer. Both programs were developed by the SPECMAP group, kindly provided by J. Imbrie and adapted for Atari ST by U. Pflaumann (Geologisch-Paläontologisches Institut, Universität Kiel). From the pollen data set, 118 data points were linearly interpolated at 5 k.y. for the interval from 80 to 665 k.y. From all curves, mean and linear trends were removed and a prewhitening constant of 0.5 was set. Frequencies were scanned from 0.001 to 0.066 with a step of 0.001 using a band width of 80 lags. The level for the confidence intervals was set at 80%. Significant frequencies were determined with a window-closing technique (Pisias et al., 1973) that used a wide band width of 15 lags and a narrow one of 80 lags.

## DIFFERENT POTENTIAL OF SITES 661 AND 658

There are large differences in the sedimentation rate between the two sites. Site 661 has a sedimentation rate of 1.5 cm/k.y. for the upper 63 m and 0.4 cm/k.y. for the interval between 63 and 82 m, while Site 658 has a rate of 15 cm/k.y. in the upper 100 m (Ruddiman, Sarnthein, et al., 1988).

Pollen concentrations of at least 50 grains per sample were found for the first 20 m of Hole 661A, but very few pollen grains were recovered below this depth (about 1.3 Ma). Bonnefille et al. (1982) report that most Pliocene levels from Deep Sea Drilling Project (DSDP) Site 367, located in the Cape Verde basin north of Site 661, are devoid of pollen, too.

The pollen assemblage in the upper 20 m of Site 661 is comparable with that found by Hooghiemstra and Agwu (1988) in meteor core M 16415-2 nearby. The large sample spacing (1 per 100 k.y.) prevents a close comparison of the results from Site 661 with those from Site 658. At Site 661, between 13 and 20 m (about 800–1300 k.y.), pollen of

*Podocarpus* were found. The occurrence of *Podocarpus* in the middle Pleistocene of tropical western Africa has also been found by Morzadec-Kerfourn (1988). She reports the disappearance of *Podocarpus* after isotope stage 16 from the sediments of a marine core at 9°N and 17°W.

The oxygen isotope curve at Site 658 provides a high-resolution stratigraphy and a good time scale. In addition, the high sedimentation rate and abundant pollen grains make Site 658 ideal for detailed research on vegetation, wind systems, and aridity of northwestern Africa during the last 3.5 Ma. For these reasons, the rest of this paper examines the palynological data from Site 658.

## DATING AND STRATIGRAPHY OF SITE 658

A detailed oxygen isotope record (resolution about 2600 yr) has been obtained for a Pleistocene section at Site 658 down to the base of isotope stage 17. Specimens of the planktonic foraminifer *Globorotalia inflata* and the benthic foraminifer *Cibicidoides wuellerstorfi* were used for oxygen isotope analyses (see Fig. 1).

The time scale for the last 670 k.y. is based on biostratigraphic data (Shipboard Scientific Party, 1988) and on the isotopic stratigraphy of Imbrie et al. (1984) and Martinson et al. (1987) with the graphical correlation technique of Pisias et al. (1984) and Prell et al. (1986). This technique requires the identification of unique isotopic events correlated into a standard oxygen isotope taxonomy. Further information and details of the oxygen isotope record of Site 658 are given in Sarnthein and Tiedemann (this vol.).

## CLUSTERING AND INTERPRETATION

We clustered the record into six pollen groups: A to F (see also Fig. 1 and Appendix A).

Group A contains Cyperaceae; taxa from swamps and wet localities, including *Rhizophora* (mangrove); and pollen from the Sudanese and Guinean Savanna (group 5 and 6 of Agwu and Beug, 1982). All these elements are favored by humid conditions.

The family of Cyperaceae has many representatives in wetter habitats and swamps, and the isopollen map for Cyperaceae (Hooghiemstra et al., 1986) shows a river-dependent component.

Apart from humid areas, Cyperaceae are also important at the boundary between the Sahara and the Sahel (Cour and Duzer, 1976; Schulz, 1987). Transport of Cyperaceae pollen by the AEJ will be important when the Sahel-Sahara boundary has shifted to the north during more humid times. The effect of vegetation types rich in Cyperaceae growing in the trajectory of the AEJ will therefore amplify the effect of the extension of humid areas producing Cyperaceae pollen grains.

Pollen grains of *Rhizophora* are probably transported by water to a great extent (Hooghiemstra et al., 1986). Periods with higher values of the mangrove pollen speak for a more humid climate. Mangrove swamps in deltas are, moreover, an indication of heavier river runoff.

Group B consists of Poaceae (grasses). This family has representatives in almost all biotopes, but they are especially abundant in the savanna. The isopollen map of recent marine material for Poaceae reflects mainly the position of the savannas of the Sudan and the Sahel (Hooghiemstra et al., 1986).

Group C contains desert elements from Sahara and Sahel. It includes Chenopodiaceae-Amaranthaceae from the Sahara and Sahel (Lezine, 1987); *Calligonum* mainly from the Sahara (Cour and Duzer, 1976; Rossignol-Strick and Duzer, 1979; White, 1983); and Capparidaceae mainly from the Sahel and the Sudanese savannas (Rossignol-Strick and Duzer, 1979; Maley, 1983; Lezine, 1987).

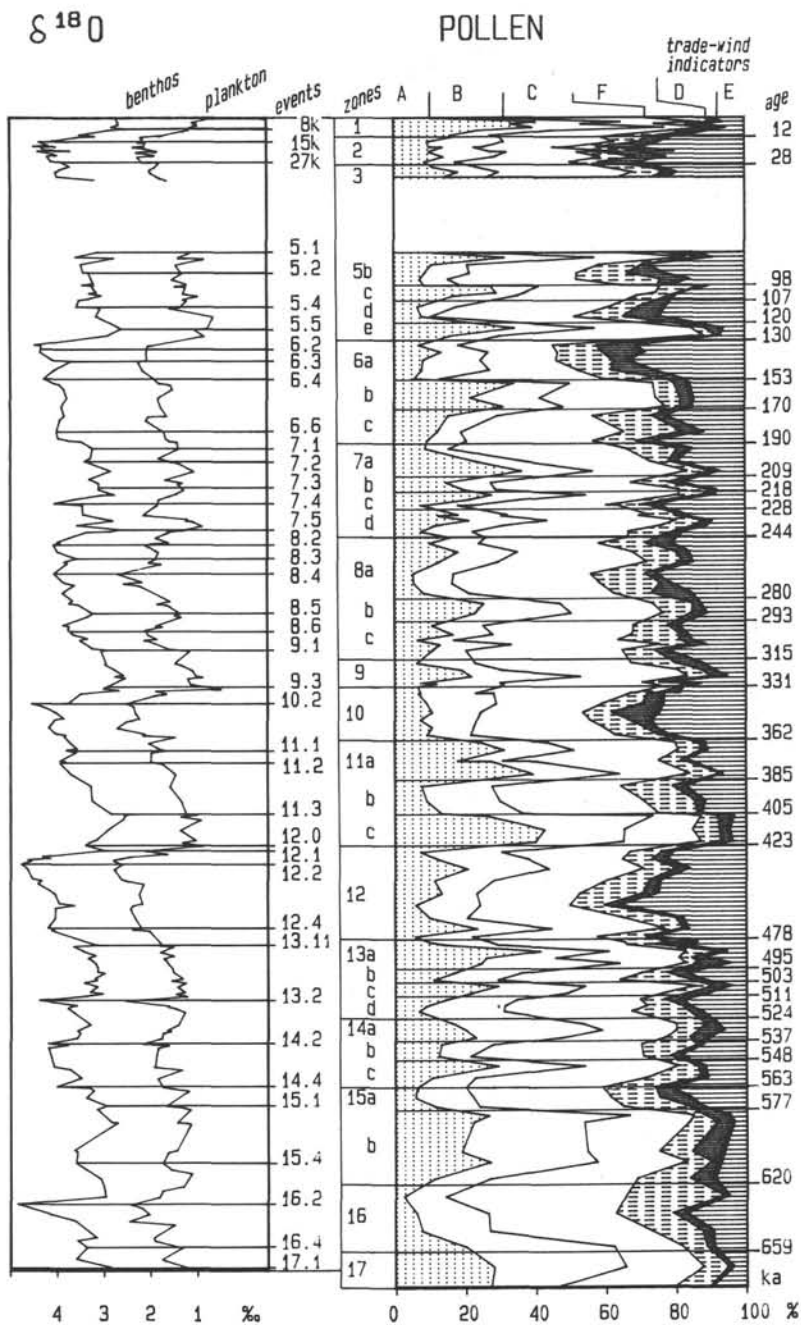


Figure 1. Oxygen isotope data and summary pollen diagram of Site 658. Isotope data (left) were measured on *Globorotalia inflata* (plankton) and *Cibicidoides wuellerstorfi* (benthos). On the horizontal axis the isotope values are expressed in per mil. Most of stages 3 and 4 are missing. The identified isotopic events are indicated. In the pollen diagram (right), all taxa recognized have been included in one of the following groups: A, humidity indicators (including Cyperaceae and *Rhizophora*); B, Poaceae; C, elements from Sahara and Sahel (including Chenopodiaceae-Amaranthaceae); D, European and Mediterranean elements; E, dry elements from the southern Mediterranean and northern Sahara (including Asteraceae and *Ephedra*); and F, other taxa. On the horizontal axis, these groups are arranged according to their indicator value of arid conditions from negative (A) to positive (E) and expressed as percentages of the total pollen count. Groups D and E together form the trade-wind indicators. The pollen curves are expressed as percentages of the total pollen count. The zones are indicated at the left of the pollen summary diagram, and their boundaries are indicated by horizontal lines. Vertical axis = time plotted linearly in k.y. The time scale is based on biostratigraphic data and oxygen isotope stratigraphy.

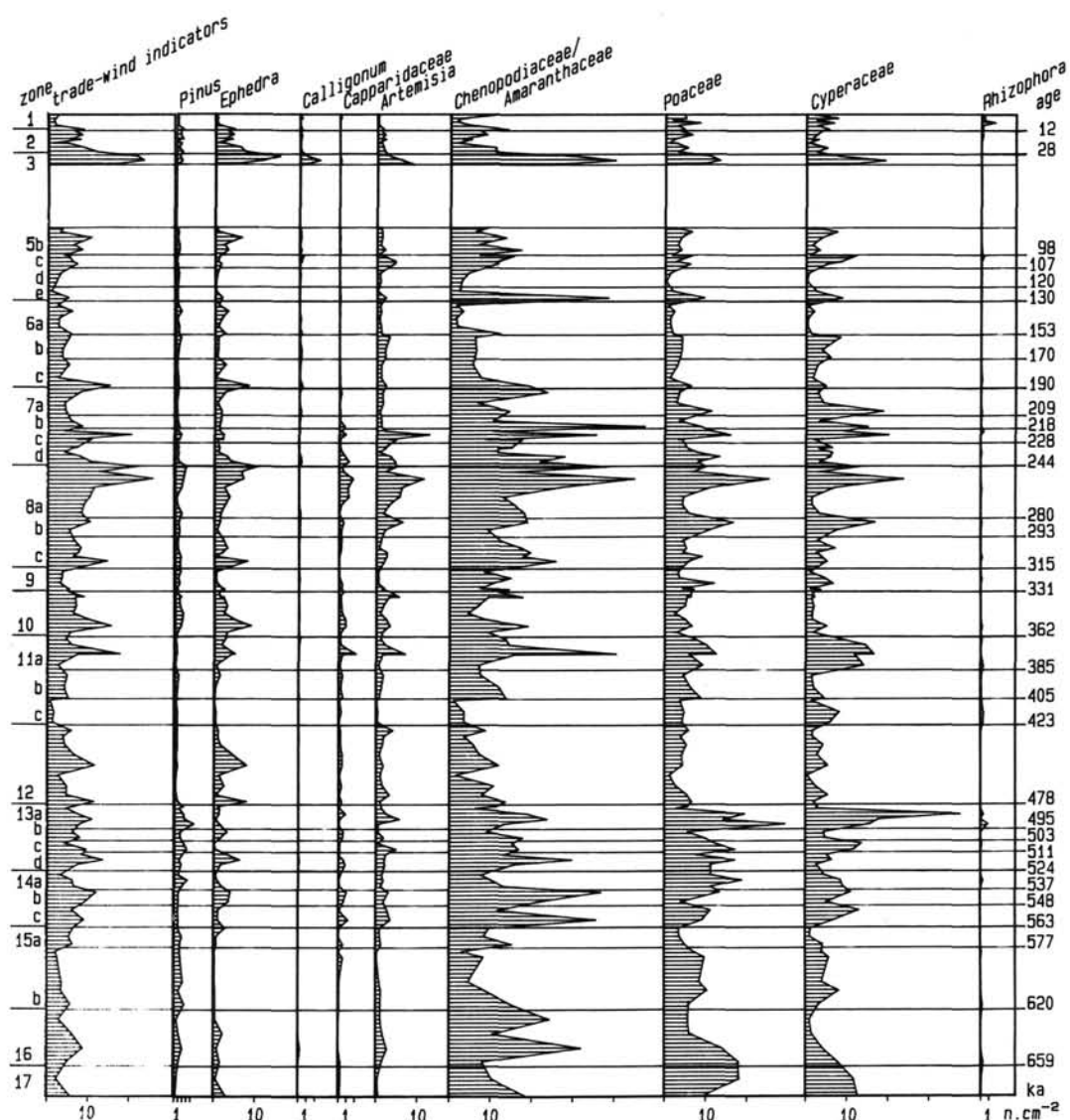


Figure 2. Pollen influx diagram of selected taxa from Site 658. Horizontal axis = influx values plotted in numbers per  $\text{cm}^3$  and year. Vertical axis = time plotted in k.y. (see also Fig. 1).

At present Chenopodiaceae-Amaranthaceae, Poaceae, and Cyperaceae are successively important in vegetation of the central or southern Sahara southward toward the area of tropical forests. The AEJ will register the shifting of those vegetation types into its source area.

Group D contains pollen types coming from Europe (mainly *Pinus* pollen) and the Mediterranean area (group 1 and 2 of Agwu and Beug, 1982).

Group E contains elements from dry communities in the southern Mediterranean and northern Sahara. It includes *Artemisia* and other Asteraceae (Compositae), both mainly from the Mediterranean (vegetation zones VII and XVIII of White, 1983), and *Ephedra*, mainly from the northern Sahara (vegetation zones VII, XVII, and XVIII of White, 1983).

In addition, we use the term "trade-wind indicators," as proposed by Hooghiemstra (1988b) and Hooghiemstra et al. (1987). That term covers pollen of *Pinus*, *Ephedra*, and Asteraceae (including *Artemisia*), all of which are pollen taxa that are supposed to be transported exclusively by the northeast trade winds to core sites off the West African coast. The

majority of pollen grains in Groups D and E are formed by these trade-wind indicators.

In Figures 2 and 3, a selected number of pollen curves is presented. We show curves of "Site 658 taxa" that are indicative of major shifts in vegetation zones, the intensity of northeast trade winds and AEJ, and river runoff.

In general, the influx diagram (Fig. 2) displays: (1) changes in the efficiency of wind transport, which is related to changes in wind speed; (2) changes in the pollen production of the vegetation within the source area; and (3) changes in the distance from the source area to the core site. For interpreting the influx diagram in terms of wind transport, it is necessary to estimate the individual contribution of the two wind systems involved (Dupont, 1989).

The percentage diagram (Fig. 3) also reflects shifting vegetation zones, as well as changes in vegetation composition.

#### ZONING OF THE DIAGRAM

The oxygen isotope record shows major fluctuations that are for the most part caused by variations in global ice volume

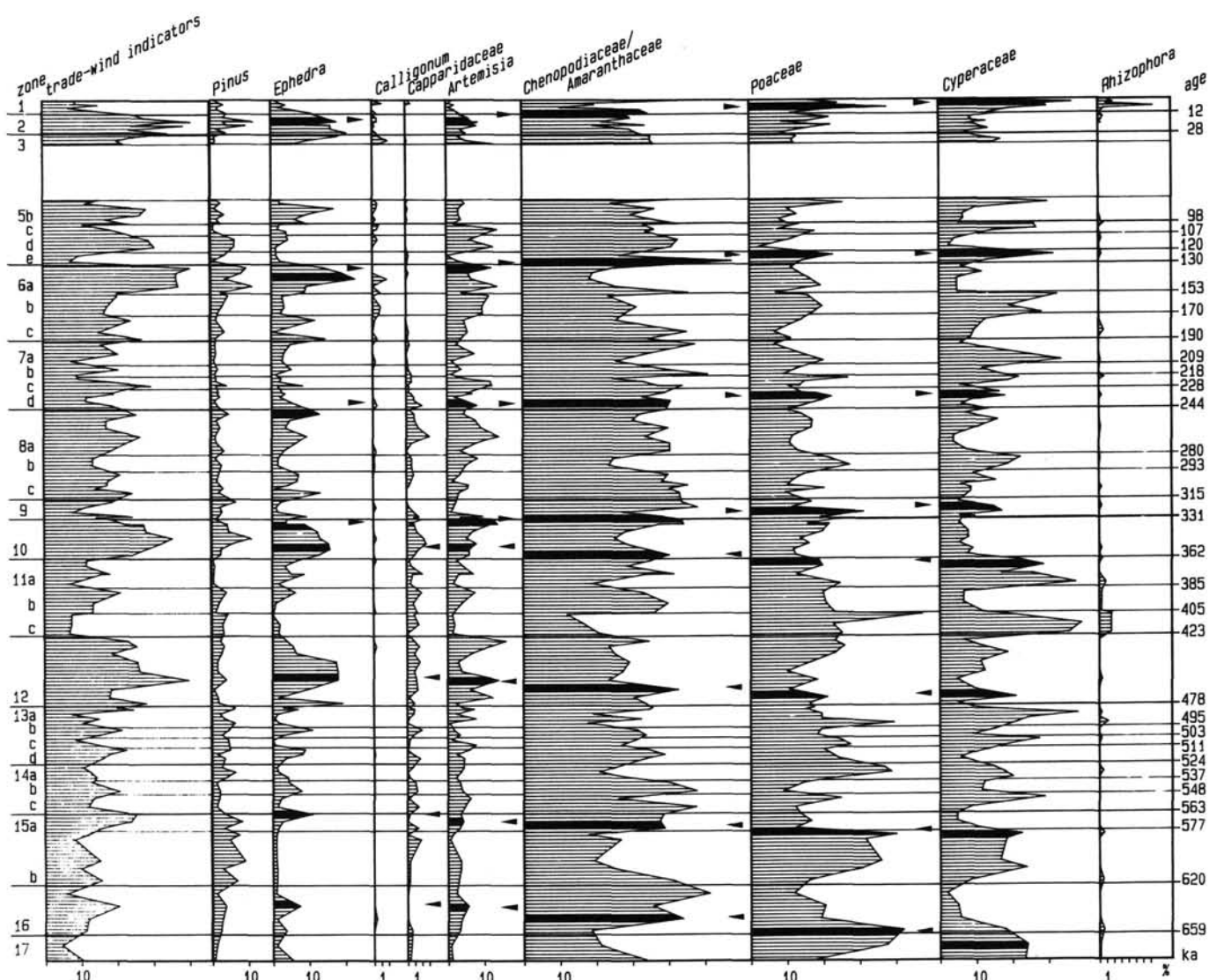


Figure 3. Pollen percentage diagram of selected taxa from Site 658. The taxa have been arranged according to their indicator value of arid (left) to humid (right) conditions, while high trade-wind indicators and high *Pinus* values indicate strong trade-wind activity. Eight cases in which subsequent maxima indicate a development from humid to arid and back are indicated by solid bars and arrows (see text). Horizontal axis = percentages of the pollen total. Vertical axis = time plotted in k.y. (see also Fig. 1).

(Labeyrie et al., 1987) and secondarily by local changes in ocean temperature. The high average rate of sediment accumulation at Site 658 (about 15 cm/k.y.) is especially advantageous for deciphering the details of climatic history because the smoothing impact of bioturbation can be largely excluded.

The palynological sequence has been described with reference to the oxygen isotope stratigraphy because of the good agreement between the fluctuations in these curves (Fig. 1). All isotope stage transitions could be recognized in the pollen diagram with the exception of those of stage 9. Zone 9 of the pollen diagram spans 331–315 k.y., while isotope stage 9 lasts from 339 to 303 k.y. This means a strongly delayed response of the vegetation to climatic amelioration at the beginning of stage 9 and an early vegetational response to climatic deterioration at the end of this stage.

The pollen diagram is divided into 34 zones. Table 1 shows a highly schematic description. The depths and ages of the zones are given. Percentages and influx values are classified as high, middle, and low. The zones are numbered

according to the isotope stages. If there are several zones in one isotope stage, the zones have been labeled with characters (stage 14, for instance, holds Zones 14a, 14b, and 14c). In some cases, several isotopic events fall within the same zone (e.g., 6a, 7a, 8a, and 11a); in two cases (13b and 13c), no isotopic event could be detected. Most of the humidity indicators (Group A) correspond with isotopic event 5.1 at the top of Zone 5b, but a separate zone has not been distinguished.

The zones are classified into two groups, "glacial" (G) and "interglacial" (I), based mainly on the relative abundance of Groups D plus E and Group A. Zones with high percentages of trade-wind indicators are grouped in drier glacial (G) zones, and those with high percentages of humidity indicators, in the more humid interglacial (I) ones. We establish four types of G and three types of I zones, described as follows.

Type II (Zones 8b, 11a, 13a, 13c, and 17) is characterized by a moderate influx of trade-wind indicators, a high-to-moderate influx of Chenopodiaceae-Amaranthaceae pollen,

**Table 1.** Zoning and classification of the pollen data.

Zone	Isotope event	Age (k.y.)	TI	Influx values C-A	P	C	TI (%)	HI (%)	Other curves	G 1	G 2	G 3	G 4	I 3	I 2	I 1	R	Depth (cm)
1	8K, 15K	12	-	-	o	o	-	+	Rh	.	.	.	.	.	2	.	23-232	
2	27K	28	o	o	-	-	+	-	Pi	1	.	.	.	.	.	.	251-607	
3	(3.1)	36	+	+	o	o	o	o	Cal	.	2	.	.	.	.	.	682-832	
Hiatus		79																
5b	5.1, 5.2	98	o	o	-	-	+	-	Rh	.	.	.	4	.	.	.	910-1182	
5c	5.3	107	o	o	-	o	o	+	Rh	.	.	.	3	.	.	.	1249-1362	
5d	(5.4)	120	-	-	-	-	+	-		1	.	.	.	.	.	.	1480-1549	
5e	5.5	130	-	+/-	o/-	o	-	+		.	.	.	.	2	.	.	1630-1699	
6a	(6.0)-6.4	153	-	-	-	-	+	-	Pi, Cal	1	.	.	.	.	.	.	1782-2058	
6b	(6.5)	170	-	o	-	o	o	+		.	.	.	3	.	.	.	2080-2207	
6c	6.6	190	-/+	-/o	-	-	o	o	Cal	1	.	.	.	.	.	.	2255-2421	
7a	7.0-7.2	209	o	o	o	+/o	o	+/o	Rh	.	.	.	4	.	.	.	2490-2640	
7b	7.3	218	o/-	+	o	o	-	o	Rh	.	.	.	3	.	.	R	2721-2790	
7c	7.4	228	+	+	+	+	+	o		.	.	3	.	.	.	.	2871-3021	
7d	7.5	244	o	+	o	-	-	o		.	.	.	3	.	.	.	3152-3379	
8a	(8.0)-8.4	280	+	+	+/-	+/-	o	-	Cap	.	.	3	.	.	.	.	3449-3899	
8b	8.5	293	o	o	+	+	-	o		.	.	.	.	.	1	R	3979-4051	
8c	8.6-9.1	315	o	o	-	-	o	-		.	.	4	.	.	.	.	4152-4477	
9	9.3	331	-	o	o	-	-	o		.	.	.	.	2	.	.	4617-4846	
10	9.3-10.2	362	o	-	-	-	+	-	Pi, Cap	1	.	.	.	.	.	.	4880-5422	
11a	11.1, 11.2	385	o	+	+	+	-	+	Rh	.	.	.	.	.	1	R	5499-5747	
11b	11.3	405	o	o	o	-	o	-	Cap	.	.	.	4	.	.	.	5841-6055	
11c	11.3-12.0	423	-	-	o	o	-	+	Rh	.	.	.	.	2	.	.	6070-6220	
12	12.0-12.4	478	o	-	-	-	+	o	Cap	1	.	.	.	.	.	.	6299-6919	
13a	(13.0), 13.11	495	o	+	+	+	-	+	Rh	.	.	.	.	.	1	R	6990-7227	
13b	?	503	o	o	o	o	o	o	Cap	.	.	.	4	.	.	.	7332-7411	
13c	?	511	o	o	+	+	-	+		.	.	.	.	.	1	.	7482-7561	
13d	13.2	524	+	+	+	o	o	-	Cap	.	.	3	.	.	.	.	7632-7760	
14a	(14.0-14.1)	537	-	-	+	o	-	o	Rh	.	.	.	.	2	.	.	7899-8049	
14b	14.2	548	+	+	o	o	o	-	Cap	.	.	3	.	.	.	.	8118-8199	
14c	(14.3-15.0)	563	o	+	o	+	-	o		.	.	.	3	.	.	.	8268-8349	
15a	15.1	577	o	o	-	-	o	-		.	.	4	.	.	.	.	8418-8562	
15b	(15.2-15.5)	620	-	-	o	o	-	o	Rh, Cap	.	.	.	2	.	.	.	8633-9136	
16	(16.0)-16.4	659	o	+	o	-	o	-	Pi, Rh	.	2	.	.	.	.	.	9279-9699	
17	(17.0)-17.1	670	-	+	+	+	-	+		.	.	.	.	1	R	9799-9898		

Note: Isotopic events correlated with the zone; those events that are not clearly shown by the isotopic record appear in brackets. Age of the lower boundary of the zone in k.y. Pollen influx values are classified into low (-), middle (o), and high (+) for trade-wind indicators (TI), Chenopodiaceae-Amaranthaceae (C-A), Poaceae (P), and Cyperaceae (C). Pollen percentage values are classified into low (-), middle (o), and high (+) for trade-wind indicators (TI) and humidity indicators (HI). Column labeled "Other curves" indicates maxima in the percentage curves of other taxa (Pi = *Pinus* curve over 10%, Cal = *Calligonum*, Cap = *Capparis*aceae, Rh = *Rhizophora*). Derived zone types (G1, G2, G3, G4, I3, I2, II; see explanation in the text) appear in column labeled "GGGGIII" and are arranged from arid to humid. R = river load expected. Depth of the upper and the lower sample of each zone appears in centimeters in the last column.

and a high influx of Poaceae and Cyperaceae (Fig. 2). This type represents warm and humid phases. The high influx of Poaceae indicates a northern position of the Sahel-Sahara boundary, probably north of 23°N. Type I1 differs from other humid types by having much larger influx values for most pollen taxa. The high pollen influx is explained by a high pollen production, produced by a denser vegetation. Most of the zones of Type I1 contain pollen grains of *Rhizophora*. This occurrence of *Rhizophora* is probably associated with pollen transport by the Senegal River.

Type I2 (Zones 1, 5e, 9, 11c, 14a, and 15b) shows a low influx of Chenopodiaceae-Amaranthaceae and trade-wind indicators, and a moderate influx of Poaceae and Cyperaceae. This type also represents a warm and humid climate, but with much less pollen production than in the Type I1 zones. The Sahel-Sahara boundary would still be at a northern position (about 23°N), comparable with its position at 9 k.y. (Hooghiemstra, 1988b). The lower influx values indicate less effective wind transport, especially of the trade winds.

Type I3 (Zones 5c, 6b, 7b, 7d, and 14c) is characterized by a higher influx of Chenopodiaceae-Amaranthaceae and by a lower influx of Poaceae. This indicates a more southern position of the Sahel-Sahara boundary than for Types I1 and I2, probably at about the same latitude as today. Therefore, Type I3 is thought to represent drier conditions.

Type G4 (Zones 5b, 7a, 8c, 11b, 13b, and 15a) is transitional between Zones G and I. It shows a moderate influx of trade-wind indicators and Chenopodiaceae-Amaranthaceae and moderate-to-low influx values for Poaceae and Cyperaceae. The Sahel-Sahara boundary is probably at about the same position as is Type I3 (and today), or a bit farther south. Trade-wind transport becomes more important, as indicated by the moderate influx of the trade-wind indicators.

Type G3 (Zones 7c, 8a, 13d, and 14b) is characterized by high influx values for most of the pollen taxa, with only the Cyperaceae showing moderate influx values. The Sahel-Sahara boundary is still at an intermediate latitude. The high influx values indicate an effective trade-wind transport and probably a high or moderate pollen production. Conditions were probably more arid than during the I2 zone, but not as arid as during the G2 zones.

In Type G2 (Zones 3 and 16), the Sahel-Sahara boundary has migrated further south, as indicated by a low influx of Poaceae. The influx of Chenopodiaceae-Amaranthaceae is still high, and the influx of trade-wind indicators is moderate. It shows rather arid conditions.

The last zone, Type G1 (Zones 2, 5d, 6a, 6c, 10, and 12), is characterized by extremely low influx values for all taxa, with the possible exception of the trade-wind indicators. For this zone type, trade-wind transport is probably strong, but the

pollen production in and north of the Sahara is extremely low, indicating very arid conditions and a southernmost position of the Sahel-Sahara boundary (at about 14°N, the same latitude as at 18 k.y.; Hooghiemstra, 1988b).

### STEPS IN THE DEVELOPMENT OF VEGETATION

The pollen taxa in Figure 3, with the exception of *Pinus* and the trade-wind indicators, are arranged according to their aridity/humidity indicator values. Time-transgressive shifts (lasting about 15 k.y.) of the successive maxima of these curves are shown.

At the transitions between Zones 17 and 16, between Zones 15b and 15a, and at the bottom part of Zone 12, a full development from wet to dry conditions is shown by the successive maxima of Cyperaceae, Poaceae, Chenopodiaceae-Amaranthaceae, *Artemisia*, and *Ephedra* (indicated by solid bars and left-pointed arrows). The development through Zones 17 and 16 spans an exceptionally long time.

At the transition from Zones 8a to 7d, 6a to 5e, and 2 to 1, a development from dry to wet conditions is shown (solid bars and right-pointed arrows). For Zone 10, which is represented by a well-developed *Ephedra* peak, there is a sequence of maxima at the beginning, which indicates a development from humid to arid conditions and then back to humid.

### RESPONSE OF THE POLLEN SIGNAL TO ORBITAL FORCING OF THE CLIMATE

The frequency spectra of the pollen data has been cross-correlated with computed variations in eccentricity, obliquity, and the precessional index (ETP data, provided by J. Imbrie; Imbrie et al., 1984). In Table 2, the main results are given for the influx curves of Poaceae (Fig. 4), Cyperaceae (Fig. 5), *Ephedra* (Fig. 6), Chenopodiaceae-Amaranthaceae (Fig. 7), and for the percentages of the trade-wind indicators (Fig. 8). Only significant frequencies are taken into account.

Cross correlation between Poaceae and Cyperaceae shows that both spectra are highly coherent. This indicates that most Poaceae and Cyperaceae pollen grains share their source area and transport mechanisms. Vegetation types with important Poaceae and Cyperaceae pollen production are probably located around the Sahel-Sahara boundary (see "Clustering and Interpretation" section, this chapter). Pollen from these regions will be transported mostly by the AEJ into the Atlantic.

Coherency spectra of Poaceae (Fig. 4) and Cyperaceae (Fig. 5) show a 40-k.y. period that corresponds with the obliquity signal. Cyperaceae lag by 4 k.y., and Poaceae by 5 k.y. This indicates a dependence of the shift of the Sahel-Sahara boundary on the tilt of the earth's axis (cf. Kutzbach and Street-Perrot, 1985; Kutzbach and Guetter, 1986). Also, the trade-wind indicators show coherence with obliquity (42 k.y.; Fig. 8) with a phase lag of 135°. Tiedemann et al. (this vol.), however, found only subordinate 40-k.y. rhythms in dust flux rates of Site 658 at 18°N.

Power spectra of *Ephedra* influx values show a maximum at 20 k.y. (Fig. 6), Chenopodiaceae-Amaranthacea at 23 k.y. (Fig. 7), and the percentages of the trade-wind indicators show maxima at 23 and 18 k.y. (Fig. 8). The maximum in the Poaceae spectrum, however, is not significant. Although a precessional dependence in the response of the vegetation of the Sahara and Sahel is likely (Prell and Kutzbach, 1987), low coherences preclude meaningful estimates of phase.

Pollen of *Ephedra* and the trade-wind indicators show strong out-of-phase correlations with the glacial rhythm of 100 k.y. (Table 2). Thus, the strength of the northeast trade winds is, apart from a dependence on obliquity, probably dependent on glacial boundary conditions.

**Table 2. Significant periodicities and those that are in phase with the ETP data of five pollen curves: influx values of Poaceae, Cyperaceae, *Ephedra*, and Chenopodiaceae-Amaranthaceae, and percentages of trade-wind indicators.**

	Significant periodicities (k.y.)	Periodicities coherent with ETP data (k.y.)
Poaceae	143 (167–125)	—
	40 (42–38)	at 42 phase shift $-49^\circ \pm 10$ (5 k.y.)
	17 (17–16)	—
Cyperaceae	59 (63–53)	—
	40 (42–38)	at 42 phase shift $-35^\circ \pm 6$ (4 k.y.)
	100 (100–91)	at 91 negatively correlated phase shift $180^\circ \pm 8$
<i>Ephedra</i>	53 (56–50)	—
	33 (32)	—
	20 (21–20)	—
Chenopodiaceae/Amaranthaceae	333 (333–250)	—
	29 (31–29)	—
	23 (23–22)	—
Trade-wind indicators (%)	100 (125–91)	at 83 negatively correlated phase shift $187^\circ \pm 17$
	42 (43–40)	at 42 negatively correlated phase shift $135^\circ \pm 18$ (5 k.y.)
	23 (23–22)	—
	18 (18)	—

Note: Periodicities are given in k.y., with the band width in parenthesis. Phase shifts are given in degrees, with the confidence interval given at the 80% level. The time lag that the pollen signal is behind the ETP curve appears in parentheses.

Ruddiman et al. (1986) showed significant 31-k.y. power in sequences from the North Atlantic, and Pisias and Rea (1988) found a significant 31-k.y. power in the equatorial Pacific. These authors give different possible explanations of the 31-k.y. frequency, but they do agree that the phenomenon is real.

Our *Ephedra* frequency spectrum shows maxima at both 33 and 53 k.y., while the Chenopodiaceae-Amaranthaceae only show a 29-k.y. power maximum, and the Cyperaceae show power at 59 k.y. This indicates that the 31-k.y. and 54-k.y. frequencies have different sources. The 54-k.y. frequency may have something to do with ice-sheet rhythms (Ruddiman et al., 1986), while the 31-k.y. may be a high-order frequency amplified by resonance in the climate system (Pisias and Rea, 1988).

### LONG-TERM CHANGES DURING THE BRUNHES EPOCH

Apart from the "high-frequency" fluctuations described by the zoning and the spectral analysis, many basic differences are detected between the lower and upper parts of the sequence.

1. Zones of Type I1, with the most humid conditions, only occur before 280 k.y.
2. The Poaceae pollen abundance shows a long-term decline, with maxima over 40% only before 300 k.y.
3. Stages 8 and 14 are surprisingly mild for glacial stages, with no severe aridity as in the zones of Type G1 or G2.
4. Strong glacial fluctuations (G1 zones) are only found after 480 k.y.
5. The Sahelian Capparidaceae occur almost exclusively before, and the Saharan *Calligonum* after, 200 k.y. Both taxa are found in the colder and drier stages.
6. The amplitude of variations of the trade-wind indicator percentages gradually increases with time.

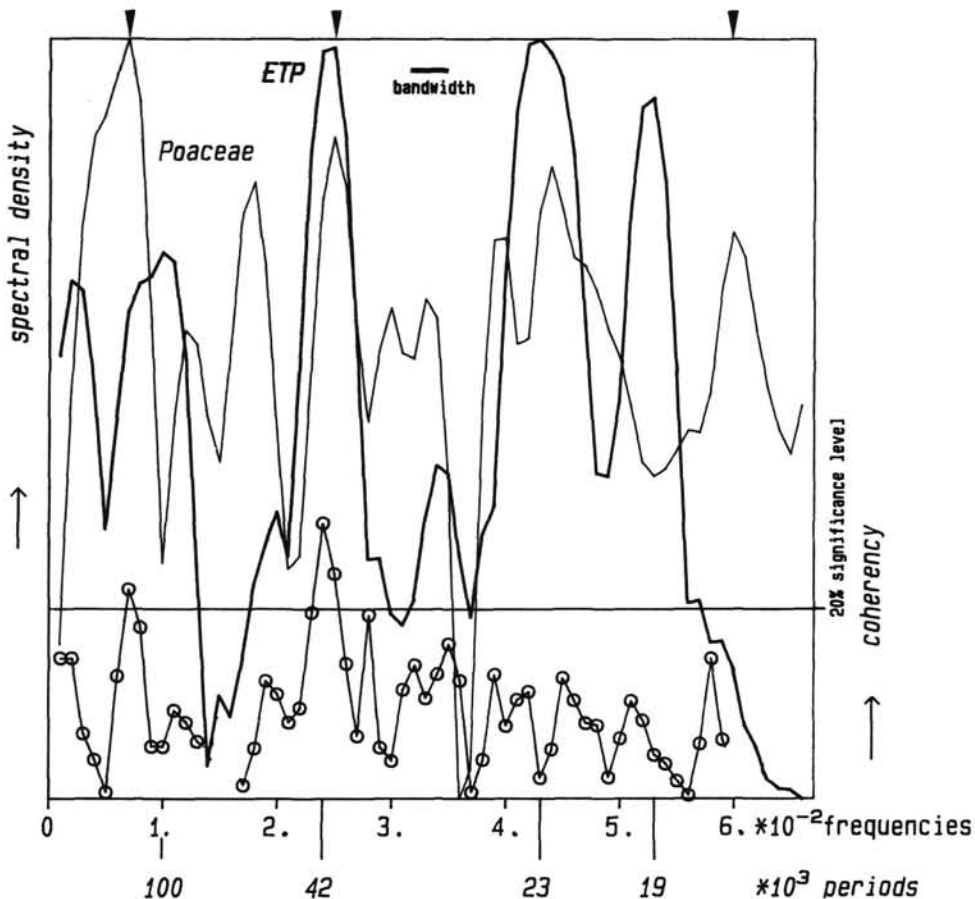


Figure 4. Frequency (upper part) and coherency (lower part) spectrum for influx values of Poaceae pollen from Site 658 with ETP data. Coherency is plotted on an arc-tangent hyperbolic scale. The horizontal line represents the 20% significance level for coherency. Power is plotted on a relative log scale (thin line for Poaceae, thick line for ETP). The frequency maxima that are significant according to the window closing technique are indicated by arrows at the top of the figure. Frequencies are plotted linearly. Band width is indicated by a horizontal bar. Periodicities belonging to "eccentricity" (100), obliquity (42), and precession (23, 19) are labeled in k.y.

From these data, we conclude that the intensity of the humid interglacial stages decreased after 280 k.y. and the intensity of the arid glacial stages increased after 480 k.y.

Several authors report a change in the paleoclimatic record at 0.4 or 0.3 Ma (Schramm, 1985; Pisias and Rea, 1988). Climatic deterioration in the late Quaternary is reported for the Northern Hemisphere and amelioration for the Southern Hemisphere and the equatorial regions (Jansen et al., 1986; Chuey et al., 1987). The pollen data of Site 658, however, indicate a trend toward stronger glacial stages and weaker interglacial stages during the younger part of the Brunhes Epoch.

The Sahel-Sahara boundary in some of the early humid interglacial stages was probably north of the position that was found for the early Holocene (9 k.y.). This would imply that the area with extremely arid vegetation types must have been very restricted or even nonexistent during such times in northwest Africa.

#### CORRELATION BETWEEN THE SITE 658 AND THE TENAGHI PHILIPPON SEQUENCE

We compare pollen data of Site 658 with those of the long terrestrial sequence from northern Greece (Tenaghi Philippon: Wijmstra and Smit, 1976; Wijmstra and Groenhart, 1983; and Wiel and Wijmstra, 1987a, 1987b). The Tenaghi Philippon

pollen sequence (Fig. 9) covers the period from the Holocene through the middle Pleistocene down to isotope stage 23 and has been analyzed at a high time resolution (closer than 1 sample per k.y.). The authors date their sequence by correlating with marine isotope stages and by the establishment of the position of the Brunhes-Matuyama boundary and the Jaramillo Event.

The correlation between Site 658 and Tenaghi Philippon is eased by the fact that aridity is an outstanding climatic factor during glacial stages in both areas. During glacial stages, a broad Saharan desert belt under an arid climate extended far northward into the present Mediterranean and North Africa, and southward into the savanna. In northern Greece, the arid climate during cold periods resulted in a predominantly steppe environment with much reduced growth of trees.

In both sequences, long-lasting and extremely arid climatic conditions prevailed during stages 16, 12, 10, and the lower part of stage 6. Furthermore, sharp climatic changes occurred across several stage transitions: 17/16, 13/12, 12/11, 11/10, and 10/9. Stage 14 displays rather mild aridity for an even isotope stage in both regions.

For the odd stages, periods with main occurrences of evergreen oaks in the Mediterranean partly correspond with zone Type II at Site 658 (11a and 13c). In the Mediterranean,

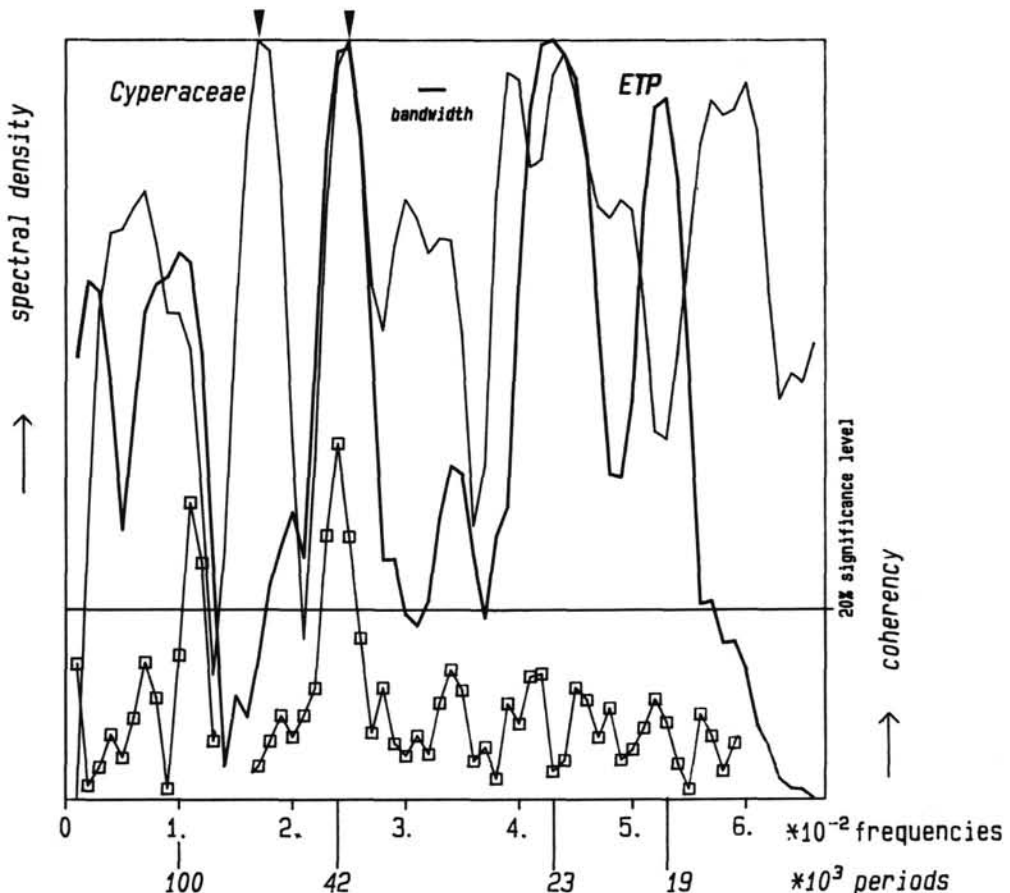


Figure 5. Frequency (upper part) and coherency (lower part) spectrum for the influx values of Cyperaceae pollen from Site 658 (thin line) with ETP data (thick line). Also see caption for Figure 4.

evergreen oaks indicate comparatively dry summers. For the Saharan region, zone Type II indicates higher or more regular rainfall probably during summer time. This emphasizes the contrast between the responses of the Mediterranean and the tropical climate system to globally warmer conditions.

### CONCLUSIONS

Sediments from Site 661 are suitable for pollen analysis in the upper 20 m (last 1.3 Ma). Below this depth pollen concentrations are too low for reliable analyses.

Sediments from Site 658 have high accumulation rates and high pollen concentrations. Isotope stratigraphy provides a detailed time scale. The following conclusions can be drawn from a pollen analysis of the upper 100 m (last 680 k.y.).

A good agreement exists between the oxygen isotope record and the percentage curves of Group A (Cyperaceae, taxa from swamps and wet localities, and from the Sudanese and Guinean savanna). The percentages of trade-wind indicators (*Pinus*, *Ephedra*, *Artemisia*, and other Asteraceae) show a negative correlation with oxygen isotopes.

Cyperaceae pollen probably have an important source area at the Sahel-Sahara boundary, as well as in swamps and wet localities in other parts of northwest Africa. The high coherency between the spectra for Poaceae and Cyperaceae pollen confirms the sharing of source localities (Sahel-Sahara boundary) and transport systems (i.e., AEJ).

Time-transgressive shifts of successive maxima of *Ephedra*, *Artemisia*, Chenopodiaceae-Amaranthaceae, Poaceae, and Cyperaceae show a gradual increase or decrease in overall humid-

ity. Eight shifts, most of them lasting about 15 k.y., are recognized in the percentage diagram.

The pollen influx diagram shows large fluctuations. They are explained in terms of wind vigor and pollen production. Arid glacial periods showed sparse vegetation in large parts of northwest Africa and very low pollen production. A probable strong northeast trade wind resulted in high percentages, but low influx values, of trade-wind indicators.

The more humid interglacials had a high pollen production. The high influx of Poaceae indicates a northern position of the Sahel-Sahara boundary. The low percentages of trade-wind indicators suggest weak northeast trades.

Intermediate to these extremes, five additional zone types are recognized in the pollen diagram, indicating variations in humidity, latitude of the Sahel-Sahara boundary, vigor of the northeast trade winds, and AEJ.

The Sahel-Sahara boundary probably shifted many times during the last 680 k.y. between 14°N and north of 23°N (Fig. 10). The estimated variations in humidity and northeast trade-wind intensity are depicted in Figure 10.

The main occurrences of evergreen oaks in the eastern Mediterranean partly correspond with our humid interglacial stages 11a (385–362 k.y.) and 13c (511–503 k.y.). Very arid conditions in both northwest Africa and the Mediterranean prevailed during isotope stages 16, 12, 10, and the lower part of stage 6.

Strong 42-k.y. power, coherent with the ETP curve, is found in the spectra of trade-wind indicator percentages and the influx of Poaceae and Cyperaceae. The influx curves of

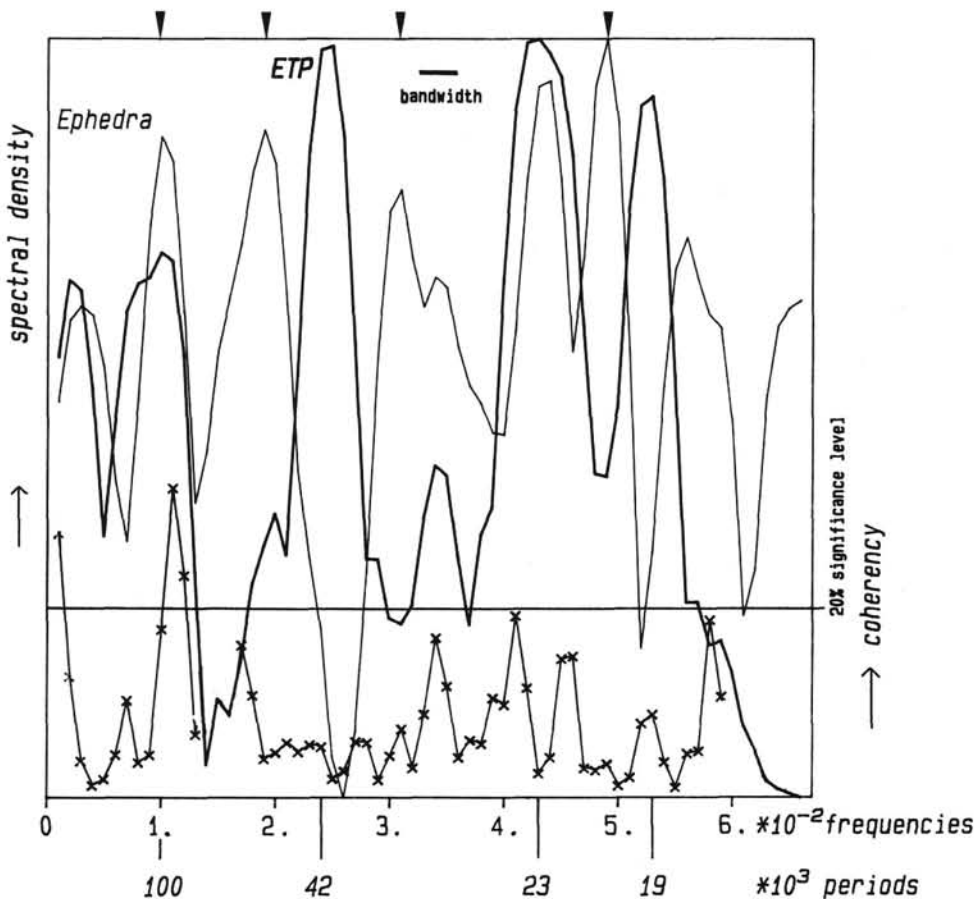


Figure 6. Frequency (upper part) and coherency (lower part) spectrum for the influx values of *Ephedra* pollen from Site 658 (thin line) with ETP data (thick line). Also see caption for Figure 4.

*Ephedra* and the percentages of trade-wind indicators show a strong 100-k.y. rhythm that is also coherent with ETP. A 23-k.y. power, although not coherent with ETP, is found for the Chenopodiaceae-Amaranthaceae influx and the trade-wind indicator percentages.

In addition, the Chenopodiaceae-Amaranthaceae influx frequency spectrum shows power at 29 k.y., while that of *Ephedra* shows power at both 33 and 53 k.y. The intensity of the humid interglacial stages decreased after 280 k.y., and the intensity of the arid glacial ones increased after 480 k.y.

#### ACKNOWLEDGMENTS

The authors wish to express their thanks to H. Hooghiemstra, U. Pflaumann, W. F. Ruddiman, M. Sarnthein, and T. Tetzlaff for fruitful discussions and suggestions; to C.O.C. Agwu for identifying pollen grains; to U. Jaschinski for preparation of the samples, and to H. Steffan for help at plotting.

The authors are indebted to the members of the Ocean Drilling Project and the shipboard party for supplying the samples, to J. Imbrie (SPECMAP) for providing us with the computer programs CROSPEC and SPECTDF and the ETP data, and to U. Pflaumann for the use of his programs (AGER and ANTPOL) and his translations of CROSPEC and SPECTDF for the Atari ST.

Financially, the project is made possible by the Bundesministerium für Forschung und Technologie (Grant KF 2004/1).

#### REFERENCES

- Agwu, C.O.C., and Beug, H.-J., 1982. Palynological studies of marine sediments off the West African coast. *Meteor Forschungsergebnisse, Reihe C*, 36:1–30.

Bonnefille, R., and Riollet, G., 1980. *Pollens des savanes d'Afrique orientale*. Paris (CNRS).

Bonnefille, R., Rossignol-Strick, M., and Riollet, G., 1982. Organic matter and palynology of DSDP Site 367. Pliocene-Pleistocene cores off West Africa. *Oceanol. Acta*, 5:97–104.

Caratini, C., Bellet, J. and Tissot, C., 1979. Etude microscopique de la matière organique: palynologie et palynofaciès. In Arnould, M., and Pelet, R. (Eds.), *La géochimie organique des sédiments marins profonds: mission ORGON III (Mauritanie, Sénégal, îles du Cap Vert)*. Paris (CNRS), 215–247.

Chuey, J. M., Rea, D. K., and Pisias, N. G., 1987. Late Pleistocene paleoclimatology of the central equatorial Pacific: a quantitative record of eolian and carbonate deposition. *Quat. Res.*, 28:323–339.

Cour, P., and Duzer, D., 1976. Persistance d'un climat hyperaride au Sahara central et méridional au cours de l'holocène. *Rev. Géogr. Phys. Geol. Dyn.*, Ser. 2, 18:175–198.

Dupont, L. M., 1989. Palynology of the last 700,000 years of Site 658 (off northwest Africa): fluctuations in paleowind systems. In Leinen, M., and Sarnthein, M., *Paleoclimatology and Paleometeorology: Modern and Past Patterns of Global Atmospheric Transport*. NATO ASI Series, Ser. D.

Hooghiemstra, H., 1988a. Palynological records from northwest African marine sediments: a general outline of the interpretation of the pollen signal. *Philos. Trans. R. Soc. London, Ser. B*, 318:431–449.

\_\_\_\_\_, 1988b. Changes of major wind belts and vegetation zones in northwest Africa 20,000–5,000 yr B.P. as deduced from a marine pollen record near Cap Blanc. *Rev. Palaeobot. Palynol.*, 55:101–140.

\_\_\_\_\_, 1989. Variation of the northwest African trade wind regime during the last 140,000 years: changes in pollen flux evidenced by marine sediment cores. In Leinen, M., and Sarnthein, M., *Paleoclimatology and Paleometeorology: Modern and Past Patterns of Global Atmospheric Transport*. NATO ASI Series, Ser. D.

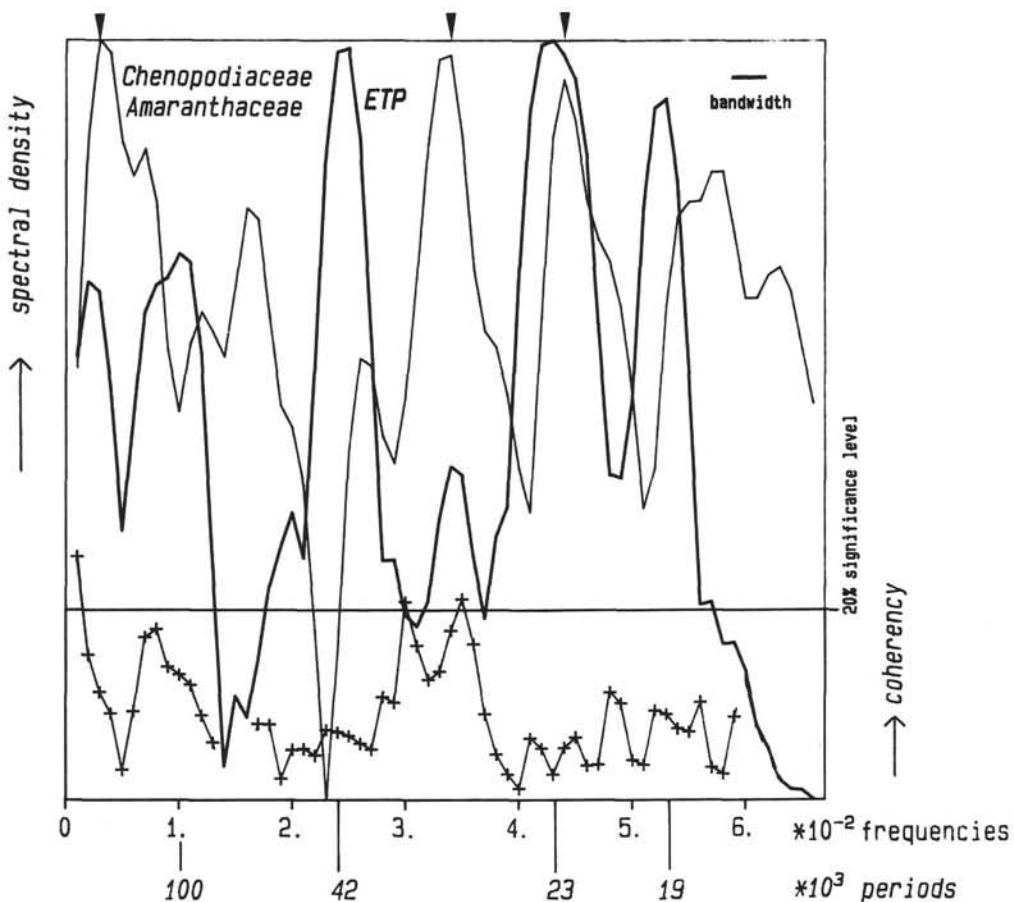


Figure 7. Frequency (upper part) and coherency (lower part) spectrum for the influx values of Chenopodiaceae-Amaranthaceae pollen from Site 658 (thin line) with ETP data (thick line). Also see caption for Figure 4.

Hooghiemstra, H. and Agwu, C.O.C., 1988. Changes in the vegetation and trade winds in equatorial northwest Africa 140,000–70,000 yr B.P. as deduced from two marine pollen records. *Paleogeogr., Palaeoclimatol., Palaeocol.*, 66:173–213.

Hooghiemstra, H., Agwu, C.O.C., and Beug, H.-J., 1986. Pollen and spore distribution in recent marine sediments: a record of northwest African seasonal wind patterns and vegetation belts. *Meteor Forschungsergeb., Reihe C*, 40:87–135.

Hooghiemstra, H., Bechler, A. and Beug, H.-J., 1987. Isopollen maps for 18,000 years B.P. of the Atlantic offshore of northwest Africa: evidence for palaeowind circulation. *Paleoceanography*, 2:561–582.

Imbrie, J., Hays, J. D., Martinson, D. G., McIntyre, A., Mix, A. C., Morley, J. J., Pisias, N. G., Prell, W. L., and Shackleton, N. J., 1984. The orbital theory of Pleistocene climate. In Berger, A. L., Imbrie, J., Hays, J., and Saltzman, B. (Eds.), *Milankovitch and Climate* (Pt. 1): Hingham, MA (D. Reidel), 269–305.

Jansen, J.H.F., Kuijpers, A., and Troelstra, S. R., 1986. A mid-Brunhes climatic event: long-term changes in global atmosphere and ocean circulation. *Science*, 232:619–622.

Kutzbach, J. E., and Guetter, P. J., 1986. The influence of changing orbital parameters and surface boundary conditions on climate simulations for the past 18,000 years. *J. Atmos. Sci.*, 43:1726–1759.

Kutzbach, J. E., and Street-Perrot, F. A., 1985. Milankovitch forcing of fluctuations in the level of tropical lakes from 18 to 0 kyr BP. *Nature*, 317:130–134.

Labeyrie, L. D., Duplessy, J. C., and Blanc, P. L., 1987. Variations in mode of formation and temperature of oceanic deep waters over the past 125,000 years. *Nature*, 327:477–482.

Lezine, A.-M., 1987. Paleoenvironments végétaux d'Afrique nord-tropicale depuis 12,000 B.P. [Ph.D. thesis]. Univ. of Marseille II, France.

Maley, J., 1983. Histoire de la végétation et du climat de l'Afrique nord-tropicale au Quaternaire récent. *Bothalia*, 14:377–389.

Martinson, D. G., Pisias, N. G., Hays, J. D., Imbrie, J., Moore, T. C., Jr., and Shackleton, N. J., 1987. Age dating and the orbital theory of the ice ages: development of a high-resolution 0 to 300,000 year chronostratigraphy. *Quat. Res.*, 27:1–29.

Melia, M. B., 1984. The distribution and relationship between palynomorphs in aerosols and deep-sea sediments off the coast of northwest Africa. *Mar. Geol.*, 58:345–371.

Morzaidec-Kerfourn, M.-T., 1988. Distribution des kystes de dinoflagellés dans les sédiments pléistocène de la marge guinéenne de l'Afrique (EQUAMARGE I, 1983). *Palaeogeogr., Palaeoclimatol., Palaeocol.*, 65:201–216.

Pisias, N. G., Dauphin, J. P., and Sanctetta, C., 1973. Spectral analysis of late Pleistocene-Holocene sediments. *Quat. Res.*, 3:3–9.

Pisias, N. G., Martinson, D. G., Moore, T. C., Jr., Shackleton, N. J., Prell, W., Hays, J., and Boden, G., 1984. High resolution stratigraphic correlation of benthic oxygen isotopic records spanning the last 300,000 years. *Mar. Geol.*, 56:119–136.

Pisias, N. G., and Rea, D. K., 1988. Late Pleistocene paleoclimatology of the central equatorial pacific: sea surface response to the southeast trade winds. *Paleoceanography*, 3:21–37.

Prell, W. L., Imbrie, J., Martinson, D. G., Morley, J. J., Pisias, N. G., Shackleton, N. J., and Streeter, H. F., 1986. Graphic correlation of oxygen isotope stratigraphy application to the late Quaternary. *Paleoceanography*, 1:137–162.

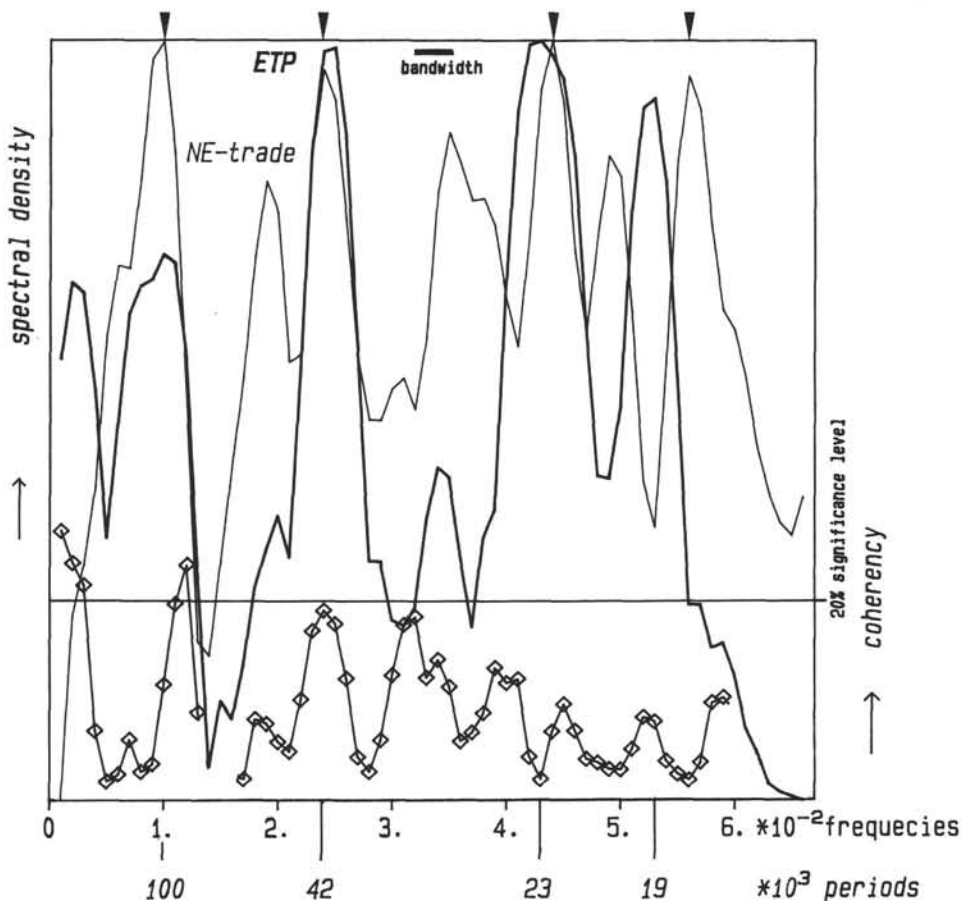


Figure 8. Frequency (upper part) and coherency (lower part) spectrum for the percentages of the trade-wind indicators from Site 658 (thin line) with ETP data (thick line). Also see caption for Figure 4.

- Prell, W. L., and Kutzbach, J. E., 1987. Monsoon variability over the past 150,000 years. *J. Geophys. Res.*, 92:8411–8425.
- Rossignol-Strick, M., and Duzer, D., 1979. Late Quaternary pollen and dinoflagellate cysts in marine cores off West Africa. *Meteor Forschungsergebnisse, Reihe C*, 30:1–14.
- Ruddiman, W. F., Sarnthein, M., et al., 1988. *Proc. ODP, Init. Repts.*, 108: College Station, TX (Ocean Drilling Program).
- Ruddiman, W. F., Shackleton, N. J., and McIntyre, A., 1986. North Atlantic sea-surface temperatures for the last 1.1 million years. In Summerhayes, C. P., and Shackleton, N. J. (Eds.), *North Atlantic Palaeoceanography*. Geol. Soc. Spec. Publ. (London), 21:155–173.
- Sarnthein, M., and Koopmann, B., 1980. Late Quaternary deep-sea record on northwest African dust supply and wind circulation. *Palaeoecol. Africa*, 12:239–253.
- Sarnthein, M., Thiede, J., Pflaumann, U., Erlenkeuser, H., Fütterer, D., Koopmann, B., Lange, H., and Seibold, E., 1982. Atmospheric and oceanic circulation patterns off northwest Africa during the past 25 million years. In von Rad, U., Hinz, K., Sarnthein, M., and Seibold, E. (Eds.), *Geology of the Northwest African Continental Margin*. Berlin-Heidelberg-New York (Springer-Verlag): 545–603.
- Schramm, C. T., 1985. Implications of radiolarian assemblages for the late Quaternary paleoceanography of the eastern equatorial Pacific. *Quat. Res.*, 24:204–218.
- Schulz, E., 1987. Die holozäne Vegetation der zentralen Sahara (nord Mali, nord Niger, südwest Lybien). *Palaeoecol. Africa*, 18:143–161.
- Shipboard Scientific Party, 1988. Site 658. In Ruddiman, W., Sarnthein, M., et al., *Proc. ODP, Init. Repts.*, 108, Sect. 1: College Station, TX (Ocean Drilling Program), 105–219.
- White, F., 1983. *Vegetation of Africa: A Descriptive Memoir to Accompany the UNESCO/AETFAT/UNSO Vegetation Map of Africa*. Paris (UNESCO).
- Wiel, A. M. van der, and Wijmstra, T. A., 1987a. Palynology of the lower part (78–120 m) of the core Tenaghi Philippon II, middle Pleistocene of Macedonia, Greece. *Rev. Palaeobot. Palynol.*, 52:73–88.
- \_\_\_\_\_, 1987b. Palynology of the 112.8–197.8 m interval of the core Tenaghi Philippon III, middle Pleistocene of Macedonia. *Rev. Palaeobot. Palynol.*, 52:89–117.
- Wijmstra, T. A., and Groenhart, M. C., 1983. Record of 700,000 years vegetational history in eastern Macedonia (Greece). *Rev. Acad. Colomb. Cienc. Exactas, Fis. Nat.*, 15:87–98.
- Wijmstra, T. A., and Smit, A., 1976. Palynology of the middle part (30–78 meters) of the 120 m deep section in northern Greece (Macedonia). *Acta Bot. Neerl.*, 25:297–312.
- Ybert, J.-P., 1979. *Atlas de pollens de Côte d'Ivoire. Initiations—documentations techniques*, 40: Paris (ORSTOM).
- Date of initial receipt: 1 February 1988**  
**Date of acceptance: 21 October 1988**  
**Ms 108B-174**
- APPENDIX A**
- List of Taxa from Site 658  
Arranged in Groups A to F**
- Group A**
1. Elements from the Sudanese and Guinean savanna zone and the tropical forest: Apocynaceae, *Acalypha*, *Alchornea*, *Antidesma* type, *Berlinia*-*Isoberlina*, Bignoniacae, *Blighia*, *Boswellia*, Bombacaceae, *Borreria*, *Bridelia* type, Combretaceae, *Calycolobus*, *Canthium*, *Cassia* type, *Celtis*, *Cissus*, *Croton*, *Crudea* type, *Diospyros*, Ebenaceae pp., *Fagara*, *Gaertnera*, *Grewia*, *Hygrophila*, *Hymenocardia*, *Hypoestes* type, *Jatropha*, *Justicia*, *Leea*, *Lannea*, Meliaceae-Sapotaceae, *Macaranga*, *Morelia*, *Myrica*, Palmae (exclusive *Hyphaene* and

*Phoenix*), Phytolaccaceae, *Pavetta*, *Pterocarpus*, Sterculiaceae, *Sapium*, *Tamarindus*, *Uapaca*, Vitaceae.

2. Elements from swamps and wet locations: Alismataceae, *Isoetes*, *Myriophyllum*, *Typha*-*Sparganium*.

3. *Rhizophora*.

4. Cyperaceae.

#### Group B

Poaceae

#### Group C

1. Elements from the Sahara: Chenopodiaceae-Amaranthaceae, *Calligonum*, *Erodium*, *Gymnocarpus*, *Moltkia*, *Neurada*, *Nitraria*, Plumbaginaceae, *Paronychia*, *Plantago*, *Polycarpaea*, *Tamarix*, *Zygophyllum*.

2. Elements from the Sahel: *Balanites*, *Blepharis*, Capparidaceae (including *Boscia*, *Cleome*, *Maerua*), *Chrozophora*, *Commiphora*, *Heliotropium*, *Indigofera* type, Mimosaceae, *Mitracarpus*, Nyctaginaceae, *Phyllanthus*, *Salvadora*, *Tribulus*, *Zizyphus*.

#### Group D

Elements of dry vegetation from southern Mediterranean and northern Sahara: Asteraceae Liguliflorae, Asteraceae Tubuliflorae, *Artemisia*, *Ephedra*.

#### Group E

1. European elements: *Abies*, *Acer*, *Alnus*, *Betula*, *Cedrus*, *Corylus*, *Empetrum*, *Fagus*, *Filipendula*, *Picea*, *Pinus*, *Rumex*, *Thalictrum*, *Tilia*, *Veronica* type.

2. Mediterranean elements: *Asphodelus*, Cistaceae, *Gypsophila*, *Olea*, *Phillyrea*, *Polycarpon*, *Quercus*, *Rhus*, *Sagina*, Thymelaeaceae.

#### Group F

Others: Acanthaceae pp., Apiaceae, Boraginaceae, Brassicaceae, Campanulaceae, Caryophyllaceae pp., Celastraceae, *Convolvulus*, Cucurbitaceae, Ericaceae, Euphorbiaceae pp., *Euphorbia*, Iridaceae, Lamiaceae, Leguminosae pp., Liliaceae, Linaceae, Malvaceae, Oleaceae pp., *Polygala*, *Polygonum* reticulate type, Ranunculaceae, Rosaceae, Rubiaceae, Rutaceae.

#### Ferns.

#### Dinoflagellates.

Note: The grouping in several vegetation zones was made using Caratini et al. (1979), Rossignol-Strick and Duzer (1979), Agwu and Beug (1982), Maley (1983), White (1983), Hooghiemstra et al. (1986), and Lezine (1987).

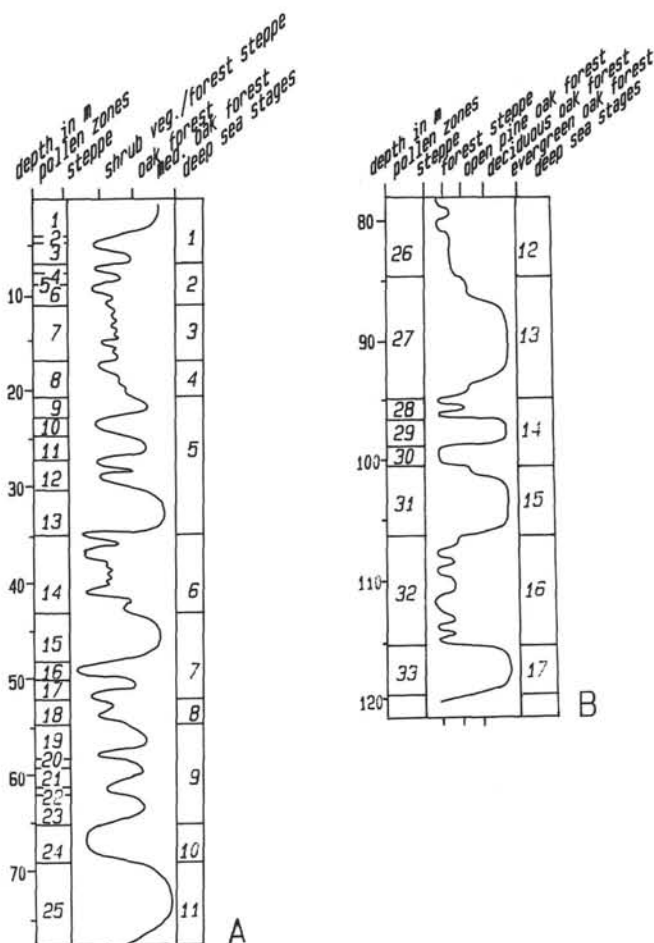


Figure 9. Diagram of different vegetation types of the Tenaghi-Philippon sequence in the eastern Mediterranean. Part A after Wijmstra and Smit (1976), adapted. The correlation between the deep-sea stages (oxygen isotope stages) and the pollen zones is after Wijmstra and Groenhart (1983). Part B after Wiel and Wijmstra (1987), adapted.

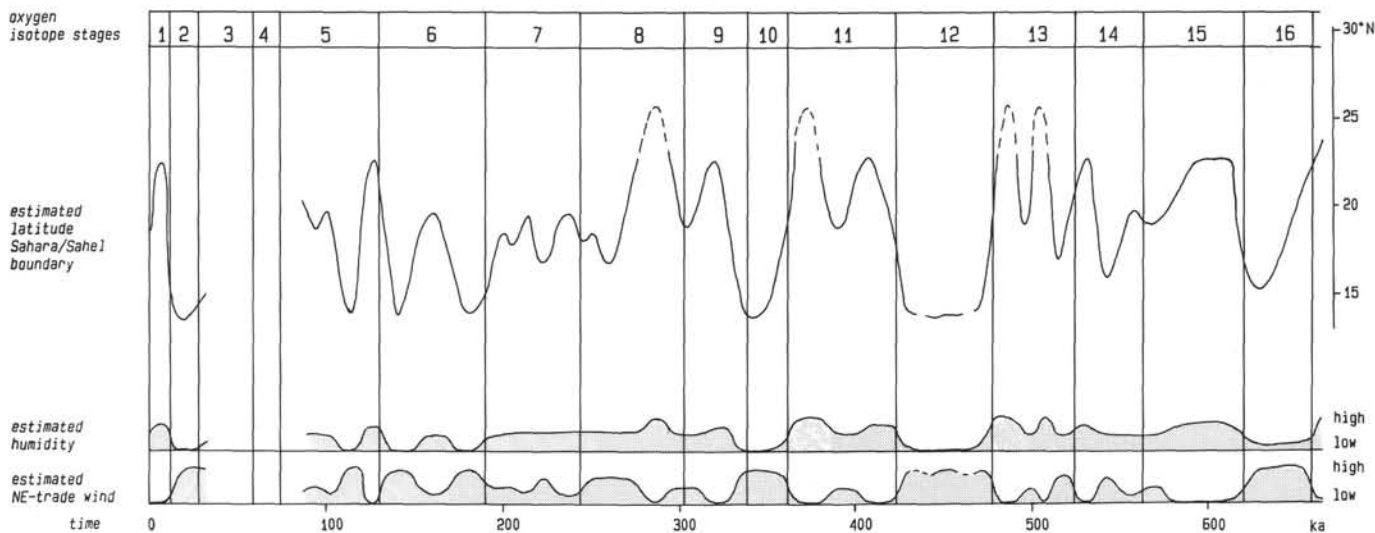


Figure 10. Summary diagram of the estimated variations in latitude of the Sahel-Sahara boundary, humidity, and northeast trade-wind vigor during oxygen isotope stages 1, 2, and 5-16 on a linear time scale.

**APPENDIX B**  
**Pollen Concentration Values of the Upper 100 Meters of Ocean Drilling Program Site 658**

Core, section, interval (cm)	Composite depth (cm)	Age (k.y.)	Sed. rate				Swamp and wet locale elements	Guinean & Sudanese savanna & tropical forest elements					
			European elements	Mediterranean elements	Saharan elements	Sahelian elements		Other elements	<i>Artemisia</i>	Asteraceae	<i>Balanites</i>		
108-658A-1H-1, 12-16	23	1	20	17.81	22.26	578.73	26.71	31.16	22.26	227.04	17.81	75.68	8.90
108-658B-2H-1, 10-14	72	4	20	29.84	9.95	192.30	6.63	19.89	26.52	49.73	6.63	29.84	0
108-658A-1H-1, 85-87	95	5	20	17.84	2.97	83.24	1.49	8.92	10.41	37.16	8.92	22.30	0
108-658B-2H-1, 76-80	138	7	20	24.75	0	116.69	3.54	7.07	21.22	31.82	7.07	28.29	0
108-658A-1H-2, 12-16	173	8	20	12.58	10.06	236.42	5.03	20.12	25.15	50.30	15.09	17.61	0
108-658B-2H-2, 20-24	232	11	21	90.86	42.76	700.17	0	42.76	37.41	245.86	69.48	48.10	0
108-658A-1H-2, 91-93	251	12	21	59.14	23.66	346.95	3.94	7.89	7.89	157.70	43.37	70.97	3.94
108-658B-2H-2, 95-99	307	15	21	60.49	21.60	432.10	4.32	4.32	17.28	99.38	86.42	51.85	0
108-658B-2H-3, 20-24	382	18	26	62.05	6.71	125.77	1.68	1.68	1.68	43.60	36.89	21.80	1.68
108-658A-1H-3, 91-93	386	18	25	31.17	25.51	198.38	0	2.83	0	155.87	76.52	42.51	0
108-658A-1H-4, 12-16	450	21	25	9.73	7.65	77.84	0	6.26	6.26	20.85	14.60	7.65	0
108-658B-2H-3, 95-99	457	21	26	46.94	9.09	98.42	0	0	0	34.83	40.88	22.71	0
108-658B-2H-4, 20-24	532	24	25	27.74	97.10	439.27	0	9.25	9.25	147.97	55.49	27.74	0
108-658B-2H-4, 95-99	607	27	26	57.11	98.98	437.81	7.61	19.04	19.04	110.40	72.33	57.11	0
108-658B-2H-5, 20-24	682	30	18	32.55	86.80	1236.90	5.42	43.40	43.40	417.73	113.93	97.65	0
108-658B-2H-5, 95-99	757	33	17	54.80	82.20	1687.78	10.96	38.36	38.36	427.42	235.63	169.87	0
108-658B-2H-6, 50-54	832	36	17	27.70	101.57	974.19	9.23	4.62	9.23	244.70	341.66	73.87	0
108-658B-2H-6, 128-132	910	79	17	20.16	116.93	548.35	24.19	4.03	4.03	161.28	56.45	96.77	0
108-658B-2H-7, 28-32	960	82	17	38.39	14.40	369.50	0	9.60	14.40	62.38	71.98	23.99	0
108-658B-3H-1, 20-24	1032	86	17	21.35	16.01	795.20	5.34	10.67	16.01	261.51	69.38	149.43	0
108-658B-3H-1, 106-110	1118	91	17	53.79	86.90	401.39	4.14	24.83	28.97	194.49	45.52	136.56	0
108-658B-3H-2, 20-24	1182	95	18	53.82	166.84	936.46	10.76	10.76	5.38	618.92	102.26	134.55	0
108-658A-3H-1, 12-16	1249	98	18	24.01	12.00	396.13	24.01	24.01	18.01	93.03	18.01	78.03	3.00
108-658B-3H-2, 94-98	1256	99	18	23.31	29.14	868.47	0	11.66	11.66	297.26	69.94	128.23	0
108-658A-3H-1, 93-97	1330	103	19	9.93	0	640.57	14.90	34.76	19.86	114.21	238.35	39.73	0
108-658B-3H-3, 50-54	1362	104	18	20.01	10.00	625.29	5.00	20.01	15.01	170.08	225.10	60.03	0
108-658A-3H-2, 93-97	1480	111	18	36.04	7.21	239.67	1.80	5.41	5.41	45.05	34.24	64.87	0
108-658A-3H-3, 12-16	1549	116	12	34.22	20.53	219.00	0	20.53	20.53	75.28	68.44	54.75	0
108-658A-3H-3, 93-97	1630	123	12	24.10	10.96	179.66	4.38	4.38	4.38	26.29	0	30.67	2.19
108-658A-3H-4, 12-16	1699	128	15	20.17	40.33	2534.28	6.72	26.89	20.17	147.89	134.44	60.50	0
108-658A-3H-4, 95-99	1782	133	16	37.82	4.58	98.55	0	1.15	1.15	45.84	44.69	14.90	0
108-658A-3H-5, 12-16	1849	137	16	80.75	38.88	188.41	5.98	5.98	2.99	128.60	56.82	32.90	2.99
108-658A-3H-5, 93-97	1930	142	17	16.42	4.11	87.58	1.37	1.37	4.11	68.42	28.74	13.68	0
108-658A-3H-6, 12-16	1999	148	12	63.73	4.11	141.85	0	4.11	4.11	53.45	78.12	14.39	0
108-658B-4H-1, 126-130	2058	153	12	66.86	48.63	1081.96	0	6.08	6.08	407.25	91.18	109.41	0
108-658A-3H-6, 93-97	2080	155	9	127.57	0	657.98	6.71	13.43	13.43	167.85	322.28	33.57	0
108-658B-4H-2, 62-66	2159	164	9	64.71	23.53	723.53	0	17.65	23.53	152.94	211.76	29.41	0
108-658A-4H-1, 20-24	2207	169	9	46.31	33.08	668.20	0	19.85	19.85	99.24	224.94	59.54	0
108-658A-4H-1, 69-71	2255	174	9	31.69	57.04	614.75	0	12.68	19.01	386.59	107.74	139.43	0
108-658A-4H-2, 12-16	2340	183	9	85.56	30.56	831.11	12.22	18.33	12.22	305.56	103.89	97.78	6.11

Core, section, interval (cm)	<i>Calligonum</i>	Capparidaceae	Chenopodiaceae/Amaranthaceae	Cyperaceae	<i>Ephedra</i>	<i>Gypsophila</i>	<i>Pinus</i>	Poaceae	<i>Rhizophora</i>	Sample volume (cm <sup>3</sup> )	Total <i>Lycopodium</i> added	Total <i>Lycopodium</i> counted	Total pollen counted
108-658A-1H-1, 12–16	0	4.45	569.83	93.49	13.36	22.26	13.36	218.14	13.36	9	12100	302	298
108-658B-2H-1, 10–14	13.26	6.63	179.04	371.34	26.52	6.63	26.52	245.35	19.89	17	21700	385	306
108-658A-1H-1, 85–87	0	0	81.76	117.43	16.35	0	14.87	81.76	4.46	18	21700	811	276
108-658B-2H-1, 76–80	0	0	113.15	321.77	21.22	0	21.22	410.17	81.33	17	21700	361	307
108-658A-1H-2, 12–16	0	0	231.39	135.81	40.24	5.03	12.58	150.90	5.03	17	12100	283	283
108-658B-2H-2, 20–24	10.69	0	673.45	261.90	219.14	37.41	80.17	219.14	5.34	20	21700	203	363
108-658A-1H-2, 91–93	0	0	346.95	185.30	141.93	15.77	51.25	165.59	0	16	21700	344	308
108-658B-2H-2, 95–99	8.64	0	423.46	116.67	207.41	17.28	51.85	311.11	8.64	18	21700	279	329
108-658B-2H-3, 20–24	3.35	0	115.71	48.63	95.59	6.71	62.05	82.17	1.68	20	21700	647	315
108-658A-1H-3, 91–93	2.83	0	195.55	113.36	155.87	17.00	31.17	79.35	0	19	21700	403	312
108-658A-1H-4, 12–16	0	0	74.37	15.29	21.55	5.56	9.73	37.53	0.70	10	12100	1741	316
108-658B-2H-3, 95–99	1.51	0	95.39	46.94	80.25	7.57	46.94	109.02	0	17	21700	843	324
108-658B-2H-4, 20–24	0	0	430.02	194.20	240.44	87.85	23.12	208.08	0	19	21700	247	313
108-658B-2H-4, 95–99	7.61	0	430.19	98.98	281.72	95.18	57.11	118.02	0	19	21700	300	357
108-658B-2H-5, 20–24	32.55	0	1204.35	320.08	607.60	70.52	32.55	434.00	0	20	21700	200	628
108-658B-2H-5, 95–99	93.16	5.48	1567.22	750.73	449.34	60.28	54.80	515.10	0	18	21700	220	810
108-658B-2H-6, 50–54	23.09	0	951.11	369.36	147.74	96.96	23.09	323.19	0	20	21700	235	568
108-658B-2H-6, 128–132	4.03	4.03	544.31	141.12	32.26	104.83	20.16	145.15	0	23	21700	234	334
108-658B-2H-7, 28–32	9.60	0	355.11	431.89	33.59	9.60	38.39	369.50	0	19	21700	238	301
108-658B-3H-1, 20–24	10.67	5.34	779.19	213.48	368.25	16.01	21.35	218.81	0	19	21700	214	400
108-658B-3H-1, 106–110	0	0	401.39	86.90	128.28	82.76	49.66	173.80	0	19	21700	276	325
108-658B-3H-2, 20–24	10.76	5.38	925.69	172.22	166.84	150.69	43.06	209.90	5.38	18	21700	224	480
108-658A-3H-1, 12–16	0	3.00	384.13	48.02	90.03	3.00	24.01	93.03	3.00	9	12100	448	299
108-658B-3H-2, 94–98	23.31	0	839.32	652.81	58.29	17.49	17.49	343.89	17.49	17	21700	219	431
108-658A-3H-1, 93–97	9.93	0	620.71	456.84	29.79	0	9.93	139.04	0	19	21700	230	344
108-658B-3H-3, 50–54	0	0	620.29	270.12	75.03	5.00	20.01	325.15	0	18	21700	241	364
108-658A-3H-2, 93–97	3.60	0	236.07	23.43	25.23	5.41	36.04	61.27	1.80	18	21700	669	306
108-658A-3H-3, 12–16	0	0	219.00	13.69	6.84	13.69	34.22	13.69	0	8	12100	221	78
108-658A-3H-3, 93–97	0	2.19	177.47	208.15	8.76	4.38	24.10	151.18	2.19	16	21700	619	303
108-658A-3H-4, 12–16	0	6.72	2514.11	571.39	107.56	6.72	20.17	618.44	0	18	12100	100	648
108-658A-3H-4, 95–99	0	0	92.82	21.77	52.71	4.58	35.52	41.25	0	18	21700	1052	319
108-658A-3H-5, 12–16	0	2.99	188.41	113.64	188.41	32.90	80.75	131.59	0	17	12100	238	327
108-658A-3H-5, 93–97	8.21	0	78.00	20.53	97.16	4.11	16.42	69.79	0	18	21700	881	310
108-658A-3H-6, 12–16	0	0	141.85	26.72	53.45	4.11	63.73	108.95	0	18	12100	327	273
108-658B-4H-1, 126–130	24.31	0	1051.57	115.49	206.67	36.47	60.78	164.12	0	17	21700	210	379
108-658A-3H-6, 93–97	0	0	657.98	899.69	80.57	0	127.57	443.13	0	16	21700	202	415
108-658B-4H-2, 62–66	23.53	0	688.24	417.65	76.47	11.76	64.71	435.29	0	17	21700	217	373
108-658A-4H-1, 20–24	19.85	0	641.74	641.74	52.93	19.85	39.70	390.34	0	16	21700	205	345
108-658A-4H-1, 69–71	6.34	0	589.40	291.53	272.52	57.04	31.69	323.22	0	16	21700	214	361
108-658A-4H-2, 12–16	0	6.11	818.89	171.11	6.11	30.56	67.22	122.22	12.22	18	12100	110	296

## APPENDIX B (continued)

Core, section, interval (cm)	Composite depth (cm)	Age (k.y.)	Sed. rate (cm/k.y.)	European elements	Mediterranean elements	Saharan elements	Sahelian elements	Swamp and wet locale elements	Guinean & Sudanese savanna & tropical forest elements	Other elements	<i>Artemisia</i>	Asteraceae	<i>Balanites</i>
108-658A-4H-2, 93-97	2421	189	15	45.28	141.50	1279.13	22.64	22.64	441.47	141.50	260.35	0	
108-658A-4H-3, 12-16	2490	193	15	35.59	106.76	1580.12	56.94	78.29	71.18	476.88	85.41	227.76	0
108-658A-4H-3, 93-97	2571	201	11	29.41	17.65	629.41	5.88	11.76	17.65	94.12	135.29	152.94	0
108-658A-4H-4, 12-16	2640	206	12	32.27	96.80	1201.93	24.20	40.33	40.33	298.47	56.47	129.07	8.07
108-658A-4H-4, 93-97	2721	213	12	44.68	25.53	880.76	19.15	63.82	31.91	229.76	82.97	210.62	6.38
108-658A-4H-5, 12-16	2790	217	17	60.50	68.06	2866.19	90.75	166.38	113.44	476.44	60.50	325.19	22.69
108-658A-4H-5, 93-97	2871	220	26	26.70	32.04	421.83	26.70	74.75	69.41	112.13	74.75	21.36	10.68
108-658A-4H-6, 12-16	2940	223	26	52.94	75.63	1406.63	60.50	52.94	45.38	294.94	491.56	158.81	22.69
108-658B-5H-1, 125-129	3020	226	25	42.87	3.06	358.25	3.06	6.12	0	88.80	116.35	42.87	0
108-658A-4H-6, 93-97	3021	226	23	28.17	11.27	777.41	22.53	33.80	16.90	152.10	202.80	202.80	5.63
108-658A-5H-1, 15-19	3152	231	23	32.16	10.72	648.64	16.08	21.44	16.08	139.38	91.13	134.02	10.72
108-658B-5H-2, 45-49	3165	232	23	21.68	13.01	511.71	13.01	26.02	21.68	134.43	91.07	95.40	0
108-658A-5H-1, 93-95	3229	235	23	35.04	10.01	495.57	65.07	20.02	15.02	110.13	30.03	75.09	40.05
108-658A-5H-2, 12-16	3299	238	23	24.20	72.60	1266.47	64.53	64.53	56.47	282.33	145.20	40.33	24.20
108-658A-5H-2, 93-95	3379	241	23	38.29	31.91	1008.41	76.59	19.15	12.76	319.12	197.85	44.68	12.76
108-658A-5H-3, 12-16	3449	245	20	138.29	138.29	1936.00	17.29	95.07	60.50	388.93	233.36	181.50	0
108-658A-5H-3, 82-85	3519	248	20	121.26	63.82	816.94	38.29	57.44	38.29	331.88	108.50	82.97	6.38
108-658A-5H-4, 12-16	3599	253	16	155.57	216.07	2912.64	181.50	121.00	77.79	1149.50	717.36	319.79	43.21
108-658A-5H-4, 93-95	3679	259	13	111.59	39.85	1976.71	119.56	47.82	39.85	502.15	454.32	95.65	23.91
108-658A-5H-5, 12-16	3749	266	10	35.59	78.29	1302.53	142.35	49.82	35.59	576.53	519.59	71.18	7.12
108-658A-5H-5, 85-87	3821	271	13	44.68	51.06	1225.41	44.68	38.29	12.76	504.21	229.76	197.85	0
108-658A-5H-6, 12-16	3899	277	13	124.39	276.41	1388.98	6.91	27.64	27.64	366.25	124.39	269.50	0
108-658A-5H-6, 93-95	3979	283	13	67.81	81.37	1437.63	74.59	135.63	135.63	651.00	474.69	142.41	13.56
108-658A-5H-7, 14-18	4051	289	13	94.11	40.33	719.28	67.22	73.94	60.50	242.00	147.89	121.00	33.61
108-658A-6H-1, 65-69	4152	296	14	40.69	27.13	881.56	40.69	20.34	13.56	210.22	74.59	176.31	13.56
108-658A-6H-2, 12-16	4249	301	18	35.59	28.47	968.00	28.47	14.24	14.24	341.65	35.59	199.29	14.24
108-658A-6H-2, 94-68	4327	304	25	38.62	27.59	788.99	16.55	11.03	11.03	297.94	99.31	82.76	5.52
108-658A-6H-3, 12-16	4395	307	25	60.50	24.20	732.05	12.10	42.35	36.30	157.30	96.80	84.70	0
108-658A-6H-3, 94-98	4477	310	25	45.68	39.97	1033.61	22.84	39.97	39.97	217.00	74.24	142.76	5.71
108-658A-6H-5, 83-87	4617	317	19	66.00	16.50	445.48	6.60	6.60	3.30	125.40	23.10	75.90	0
108-658A-6H-6, 12-16	4696	322	19	37.46	21.41	792.04	21.41	42.81	42.81	112.38	26.76	101.68	5.35
108-658A-6H-6, 83-87	4767	325	19	57.44	44.68	561.65	51.06	25.53	31.91	134.03	19.15	51.06	12.76
108-658B-7H-1, 40-44	4835	329	19	19.98	3.33	402.96	23.31	19.98	9.99	49.95	99.91	33.30	0
108-658A-6H-7, 12-16	4846	329	19	31.54	31.54	763.35	44.16	31.54	31.54	214.49	69.40	50.47	6.31
108-658B-7H-1, 115-119	4880	331	20	13.55	4.52	605.04	31.61	9.03	9.03	72.24	176.09	13.55	0
108-658A-6H-9, 5-9	4967	335	24	60.78	33.15	756.94	22.10	33.15	27.63	116.03	232.05	22.10	5.53
108-658B-7H-2, 40-44	4968	335	24	44.19	6.80	390.90	17.00	10.20	10.20	47.59	125.77	23.79	3.40
108-658A-7H-1, 76-78	5112	341	24	49.21	14.06	295.24	21.09	7.03	7.03	119.50	70.29	45.69	7.03
108-658A-7H-2, 12-16	5199	346	17	111.32	30.36	269.86	33.73	26.99	23.61	84.33	53.97	64.09	6.75
108-658A-7H-2, 85-89	5272	350	17	100.46	23.64	514.13	70.92	29.55	23.64	200.93	141.83	59.10	11.82
108-658A-7H-3, 12-16	5349	355	17	80.67	30.25	1139.42	90.75	40.33	20.17	373.08	191.58	121.00	10.08
108-658A-7H-3, 85-89	5422	359	17	30.80	13.20	541.18	17.60	13.20	8.80	162.79	79.20	44.00	0
108-658A-7H-4, 12-16	5499	364	17	14.67	29.33	806.67	14.67	14.67	7.33	154.00	58.67	44.00	0
108-658A-7H-4, 85-89	5572	368	17	30.14	24.11	861.97	30.14	42.19	42.19	198.92	126.58	90.42	12.06
108-658B-7H-6, 94-98	5646	374	12	42.19	36.17	3478.03	223.03	60.28	42.19	530.44	584.69	452.08	30.14
108-658A-7H-5, 12-16	5649	374	12	30.25	50.42	1361.25	30.25	60.50	60.50	282.33	121.00	141.17	0
108-658B-7H-7, 18-22	5747	382	13	12.76	0	536.12	25.53	19.15	25.53	255.29	44.68	95.74	6.38
108-658B-8H-1, 37-41	5841	389	13	66.89	0	562.98	61.32	11.15	11.15	250.83	128.20	55.74	5.57
108-658B-8H-1, 121-125	5956	397	13	51.06	19.15	912.68	25.53	51.06	44.68	331.88	89.35	153.18	0
108-658B-8H-2, 50-54	6055	405	13	33.91	6.78	1030.75	67.81	13.56	13.56	318.72	47.47	298.38	13.56

## FIRST PALYNOLOGICAL RESULTS FROM SITE 658: POLLEN AS CLIMATE INDICATORS

Core, section, interval (cm)	<i>Calligonum</i>	Capparidaceae	Chenopodiaceae/ Amaranthaceae	Cyperaceae	<i>Ephedra</i>	<i>Gypsophila</i>	<i>Pinus</i>	Poaceae	<i>Rhizophora</i>	Sample volume (cm <sup>3</sup> )	Total <i>Lycopodium</i> added	Total <i>Lycopodium</i> counted	Total pollen counted
108-658A-4H-2, 93–97	22.64	5.66	1250.83	311.29	532.03	124.52	45.28	407.51	0	18	21700	213	637
108-658A-4H-3, 12–16	0	14.24	1530.29	185.06	163.71	42.71	35.59	220.65	0	17	12100	100	453
108-658A-4H-3, 93–97	0	0	617.65	388.24	58.82	11.76	23.53	252.94	0	17	21700	217	306
108-658A-4H-4, 12–16	16.13	8.07	1161.60	1516.53	129.07	16.13	32.27	911.53	8.07	15	12100	100	560
108-658B-4H-4, 93–97	0	6.38	848.85	255.29	114.88	19.15	38.29	274.44	0	17	21700	200	340
108-658A-4H-5, 12–16	0	37.81	2835.94	899.94	60.50	30.25	52.94	514.25	0	16	12100	100	735
108-658A-4H-5, 93–97	0	10.68	405.81	357.75	42.72	5.34	21.36	443.18	10.68	16	21700	254	309
108-658A-4H-6, 12–16	0	30.25	1368.81	771.38	83.19	22.69	52.94	612.56	0	16	12100	100	542
108-658B-5H-1, 125–129	0	0	352.12	73.49	79.61	3.06	39.81	128.60	0	19	21700	373	307
108-658A-4H-6, 93–97	0	5.63	754.88	95.77	28.17	5.63	22.53	180.27	0	18	21700	214	305
108-658A-5H-1, 15–19	0	5.36	637.92	268.03	48.25	5.36	32.16	230.51	0	16	21700	253	306
108-658B-5H-2, 45–49	0	8.67	498.70	134.43	47.70	8.67	21.68	238.51	0	18	21700	278	306
108-658A-5H-1, 93–95	0	15.02	495.57	270.31	35.04	0	35.04	335.39	5.01	15	21700	289	300
108-658A-5H-2, 12–16	8.07	40.33	1185.80	250.07	129.07	16.13	24.20	564.67	0	15	12100	100	361
108-658A-5H-2, 93–95	12.76	51.06	970.12	146.79	178.71	12.76	38.29	357.41	0	17	21700	200	380
108-658A-5H-3, 12–16	0	17.29	1858.21	622.29	509.93	60.50	129.64	484.00	0	14	12100	100	547
108-658A-5H-3, 82–85	0	25.53	785.03	172.32	319.12	57.44	114.88	344.65	0	17	21700	200	384
108-658A-5H-4, 12–16	0	121.00	2800.29	1477.93	440.79	121.00	121.00	1581.64	0	14	12100	100	1075
108-658A-5H-4, 93–95	0	79.71	1960.76	510.12	175.35	7.97	111.59	820.97	7.97	17	27100	200	615
108-658A-5H-5, 12–16	0	121.00	1238.47	135.24	348.76	21.35	35.59	419.94	0	17	12100	100	516
108-658A-5H-5, 85–87	0	19.15	1193.50	114.88	191.47	38.29	44.68	319.12	0	17	21700	200	461
108-658A-5H-6, 12–16	13.82	0	1375.16	248.77	110.57	269.50	117.48	442.26	0	17	12100	103	490
108-658A-5H-6, 93–95	6.78	40.69	1424.06	1268.09	94.94	33.91	61.03	1254.53	6.78	16	21700	200	845
108-658A-5H-7, 14–18	6.72	20.17	699.11	551.22	47.06	13.44	80.67	806.67	0	18	12100	100	438
108-658A-6H-1, 65–69	0	20.34	854.44	196.66	155.97	13.56	40.69	311.94	0	16	21700	200	315
108-658A-6H-2, 12–16	0	14.24	960.88	384.35	170.82	7.12	35.59	284.71	0	17	12100	100	352
108-658A-6H-2, 94–68	0	5.52	777.96	99.31	77.24	16.55	38.62	176.56	0	19	21700	207	311
108-658A-6H-3, 12–16	0	0	707.85	151.25	12.10	18.15	54.45	356.95	6.05	16	12100	125	290
108-658A-6H-3, 94–98	0	0	1022.18	199.87	314.08	17.13	45.68	228.42	0	19	21700	200	415
108-658A-6H-5, 83–87	0	0	442.18	52.80	23.10	6.60	66.00	168.29	0	16	21700	411	306
108-658A-6H-6, 12–16	5.35	5.35	781.34	240.82	16.05	10.70	37.46	187.31	5.35	17	12100	133	304
108-658A-6H-6, 83–87	0	19.15	555.26	344.65	31.91	19.15	57.44	631.85	0	17	21700	200	318
108-658B-7H-1, 40–44	0	16.65	396.30	56.61	96.58	0	19.98	226.46	0	18	21700	362	308
108-658A-6H-7, 12–16	0	18.93	757.04	182.95	126.17	25.23	31.54	372.21	0	14	12100	137	306
108-658B-7H-1, 115–119	0	27.09	605.04	81.27	54.18	4.52	13.55	325.09	0	18	21700	267	307
108-658A-6H-9, 5–9	0	5.53	745.89	88.40	60.78	22.10	60.78	265.21	0	15	12100	146	305
108-658B-7H-2, 40–44	0	10.20	390.90	57.79	91.78	3.40	44.19	224.34	0	19	21700	336	306
108-658A-7H-1, 76–78	0	14.06	291.72	80.84	130.05	7.03	49.21	207.37	0	18	21700	343	298
108-658A-7H-2, 12–16	3.37	23.61	259.74	80.96	134.93	10.12	111.32	141.68	0	17	12100	211	305
108-658A-7H-2, 85–89	0	47.28	508.22	94.55	277.75	17.73	100.46	289.57	0	17	21700	216	305
108-658A-7H-3, 12–16	0	50.42	1109.17	292.42	514.25	30.25	80.67	383.17	10.08	12	12100	100	322
108-658A-7H-3, 85–89	0	13.20	541.18	101.20	171.59	8.80	30.80	167.19	0	18	21700	274	306
108-658A-7H-4, 12–16	7.33	7.33	792.00	491.33	154.00	14.67	7.33	425.33	7.33	15	12100	110	307
108-658A-7H-4, 85–89	0	18.08	855.94	849.92	102.47	12.06	24.11	590.72	0	18	21700	200	494
108-658B-7H-6, 94–98	0	174.81	3435.83	1404.47	421.94	30.14	42.19	1054.86	0	18	21700	200	1374
108-658A-7H-5, 12–16	0	30.25	1331.00	1008.33	342.83	30.25	20.17	504.17	0	12	12100	100	391
108-658B-7H-7, 18–22	0	12.76	536.12	1059.47	44.68	0	12.76	695.68	25.53	17	21700	200	443
108-658B-8H-1, 37–41	0	33.44	562.98	111.48	105.91	0	66.89	340.02	5.57	17	21700	229	305
108-658B-8H-1, 121–125	0	19.15	906.29	146.79	19.15	12.76	44.68	472.29	6.38	17	21700	200	356
108-658B-8H-2, 50–54	6.78	47.47	1023.97	339.06	6.78	6.78	27.13	657.78	6.78	16	21700	200	419

## APPENDIX B (continued)

Core, section, interval (cm)	Composite depth (cm)	Age (k.y.)	Sed. rate (cm/k.y.)	European elements	Mediterranean elements	Saharan elements	Sahelian elements	Swamp and wet locale elements	Guinean & Sudanese savanna & tropical forest	Other elements	<i>Artemisia</i>	Asteraceae	Balanites
108-658A-8H-1, 83-87	6070	406	11	32.29	2.48	91.91	9.94	24.84	27.32	37.26	9.94	14.90	2.48
108-658A-8H-2, 12-16	6149	414	10	61.01	0	359.27	47.45	40.67	40.67	162.69	40.67	13.56	0
108-658A-8H-2, 83-87	6220	421	10	54.55	5.46	354.58	16.37	16.37	16.37	92.74	21.82	10.91	10.91
108-658A-8H-3, 12-16	6299	427	13	42.69	18.30	652.57	30.49	6.10	6.10	170.77	298.84	18.30	12.20
108-658A-8H-3, 83-87	6370	431	17	28.43	11.37	213.25	22.75	5.69	2.84	73.93	102.36	42.65	2.84
108-658A-8H-4, 12-16	6449	437	14	43.02	21.51	419.47	26.89	26.89	26.89	155.96	107.56	48.40	5.38
108-658A-8H-4, 82-86	6519	444	10	33.91	47.47	712.03	54.25	0	0	284.81	67.81	94.94	0
108-658A-8H-5, 12-16	6599	451	10	73.94	114.28	1169.67	60.50	40.33	26.89	752.89	161.33	127.72	6.72
108-658A-8H-5, 83-87	6670	458	10	24.59	4.10	151.62	10.24	6.15	4.10	61.47	88.10	24.59	0
108-658A-8H-6, 12-16	6749	465	10	14.24	42.71	1039.18	35.59	7.12	7.12	348.76	149.47	49.82	0
108-658A-8H-6, 85-89	6822	472	12	36.17	0	675.11	24.11	36.17	42.19	120.56	271.25	48.22	12.06
108-658B-9H-3, 61-65	6919	476	21	37.50	12.50	650.00	31.25	0	0	262.50	43.75	87.50	6.25
108-658B-9H-3, 132-136	6990	480	21	100.05	30.01	550.25	35.02	15.01	10.00	185.09	60.03	105.05	15.01
108-658A-9H-1, 81-85	7018	481	21	55.06	11.59	307.18	14.49	2.90	5.80	69.55	63.76	40.57	0
108-658A-9H-2, 12-16	7093	485	19	112.36	34.57	993.93	129.64	112.36	121.00	466.71	129.64	86.43	77.79
108-658A-9H-2, 99-103	7164	489	19	128.84	20.34	1234.19	108.50	13.56	13.56	135.63	291.59	128.84	101.72
108-658A-9H-3, 12-16	7227	492	19	325.19	22.69	703.31	15.13	52.94	60.50	158.81	22.69	75.63	0
108-658A-9H-4, 12-16	7332	497	19	74.05	14.81	473.93	54.30	14.81	4.94	108.61	24.68	64.18	0
108-658A-9H-4, 91-95	7411	501	19	74.24	34.26	930.82	34.26	45.68	34.26	542.50	91.37	165.61	0
108-658A-9H-5, 12-16	7482	505	19	121.00	14.24	797.18	28.47	14.24	7.12	128.12	28.47	78.29	0
108-658A-9H-5, 91-95	7561	509	19	153.18	31.91	887.15	12.76	19.15	19.15	236.15	248.91	70.21	0
108-658A-9H-6, 12-16	7632	513	19	103.86	12.98	694.58	6.49	6.49	6.49	136.32	116.85	58.42	0
108-658A-9H-6, 81-85	7701	517	19	57.44	19.15	1576.44	51.06	19.15	25.53	408.47	102.12	229.76	6.38
108-658A-9H-6, 140-144	7760	520	19	83.97	12.00	827.69	65.98	23.99	17.99	395.85	107.96	113.96	6.00
108-658A-10H-1, 12-16	7899	527	19	42.18	15.82	400.70	15.82	26.36	31.63	137.08	68.54	42.18	0
108-658A-10H-1, 81-85	7968	531	19	165.94	19.15	536.12	6.38	19.15	19.15	159.56	89.35	31.91	6.38
108-658A-10H-2, 12-16	8049	535	19	90.75	45.38	695.75	15.13	30.25	30.25	158.81	52.94	98.31	7.56
108-658A-10H-2, 81-85	8118	539	17	57.44	19.15	2144.47	76.59	25.53	19.15	855.24	172.32	229.76	6.38
108-658A-10H-3, 12-16	8199	546	12	92.53	21.35	1807.88	49.82	28.47	21.35	291.82	149.47	256.24	0
108-658A-10H-3, 81-85	8268	551	12	70.21	12.76	982.88	25.53	0	0	210.62	229.76	121.26	12.76
108-658A-10H-4, 12-16	8349	558	12	96.80	32.27	2976.60	104.87	40.33	32.27	951.87	290.40	298.47	0
108-658A-10H-4, 81-85	8418	564	12	72.33	12.06	801.69	6.03	30.14	18.08	313.44	72.33	150.69	0
108-658A-10H-5, 12-16	8492	570	13	146.16	11.24	657.70	16.86	16.86	16.86	236.10	73.08	151.78	5.62
108-658A-10H-5, 84-88	8562	575	13	102.12	25.53	1167.97	63.82	25.53	25.53	555.26	95.74	229.76	6.38
108-658A-10H-6, 12-16	8633	580	14	93.20	0	226.93	4.05	20.26	16.21	44.58	16.21	28.37	4.05
108-658A-10H-6, 65-69	8686	584	14	108.50	0	596.75	74.59	27.13	27.13	176.31	13.56	40.69	33.91
108-658A-11H-2, 12-16	8920	601	14	154.37	5.51	336.31	5.51	16.54	22.05	159.88	60.65	27.57	0
108-658A-11H-3, 12-16	9004	607	14	72.33	0	622.07	14.47	21.70	14.47	173.60	86.80	57.87	0
108-658A-11H-4, 12-16	9136	617	14	176.31	13.56	1078.22	20.34	27.13	20.34	393.31	74.59	128.84	0
108-658A-11H-5, 12-16	9279	627	14	38.29	12.76	1755.15	6.38	6.38	6.38	963.74	76.59	63.82	0
108-658A-11H-6, 12-16	9420	637	14	76.59	12.76	765.88	0	25.53	19.15	338.26	114.88	82.97	0
108-658A-11H-7, 12-16	9566	647	14	134.44	33.61	2268.75	33.61	50.42	67.22	739.44	184.86	235.28	16.81
108-658A-11H-8, 12-16	9699	656	14	70.21	0	555.26	19.15	12.76	12.76	204.24	95.74	63.82	0
108-658A-12H-1, 12-16	9799	668	8	65.10	28.93	1222.43	57.87	57.87	50.63	405.07	43.40	101.27	7.23
108-658A-12H-2, 12-16	9898	680	8	36.17	14.47	2177.23	21.70	21.70	21.70	643.77	72.33	202.53	0

Core, section, interval (cm)	<i>Calligonum</i>	Capparidaceae	Chenopodiaceae/ Amaranthaceae	Cyperaceae	<i>Ephedra</i>	<i>Gypsophila</i>	<i>Pinus</i>	Poaceae	<i>Rhizophora</i>	Sample volume (cm <sup>3</sup> )	Total <i>Lycopodium</i> added	Total <i>Lycopodium</i> counted	Total pollen counted
108-658A-8H-1, 83–87	0	7.45	91.91	134.13	0	0	32.29	357.69	12.42	16	21700	546	305
108-658A-8H-2, 12–16	0	40.67	352.49	813.45	40.67	0	61.01	474.51	33.89	15	12100	119	308
108-658A-8H-2, 83–87	0	0	349.12	594.60	27.28	0	54.55	420.04	27.28	18	21700	221	306
108-658A-8H-3, 12–16	0	18.30	646.47	121.98	73.19	6.10	42.69	433.01	0	16	12100	124	307
108-658A-8H-3, 83–87	2.84	14.22	204.72	96.67	48.34	5.69	28.43	224.62	0	18	21700	424	306
108-658A-8H-4, 12–16	0	16.13	414.09	306.53	107.56	10.76	43.02	381.82	0	18	12100	125	307
108-658A-8H-4, 82–86	0	40.69	691.69	264.47	413.66	33.91	33.91	400.09	0	16	21700	200	350
108-658A-8H-5, 12–16	0	40.33	1136.06	510.89	746.17	47.06	60.50	416.78	0	18	12100	100	619
108-658A-8H-5, 83–87	0	10.24	147.52	28.68	112.69	2.05	24.59	114.74	2.05	17	21700	623	306
108-658A-8H-6, 12–16	0	35.59	1024.94	227.76	227.76	14.24	14.24	256.24	0	17	12100	100	337
108-658A-8H-6, 85–89	0	6.03	669.08	458.11	36.17	0	36.17	464.14	0	18	21700	200	364
108-658B-9H-3, 61–65	0	18.75	643.75	93.75	368.75	6.25	37.50	312.50	0	16	21700	217	306
108-658B-9H-3, 132–136	0	5.00	540.25	135.06	45.02	20.01	95.04	265.12	0	18	21700	241	304
108-658A-9H-1, 81–85	0	8.69	307.18	118.82	60.86	2.90	52.16	136.20	0	18	21700	416	305
108-658A-9H-2, 12–16	0	43.21	993.93	1961.93	60.50	8.64	112.36	1011.21	17.29	14	12100	100	598
108-658A-9H-2, 99–103	0	6.78	1234.19	922.25	20.34	0	128.84	745.94	0	16	21700	200	560
108-658A-9H-3, 12–16	0	0	688.19	816.75	68.06	0	242.00	1527.63	45.38	16	12100	100	512
108-658A-9H-4, 12–16	0	29.62	473.93	227.09	162.91	4.94	69.11	291.27	0	19	24200	258	306
108-658A-9H-4, 91–95	0	22.84	925.11	245.55	79.95	22.84	74.24	502.53	0	19	21700	200	480
108-658A-9H-5, 12–16	0	7.12	797.18	704.65	0	0	113.88	640.59	7.12	17	24200	200	363
108-658A-9H-5, 91–95	0	6.38	874.38	612.71	19.15	0	153.18	887.15	0	17	21700	200	508
108-658A-9H-6, 12–16	0	0	694.58	266.15	175.27	0	97.37	402.47	0	16	24200	233	307
108-658A-9H-6, 81–85	6.38	31.91	1563.68	331.88	325.50	12.76	57.44	899.91	0	17	21700	200	631
108-658A-9H-6, 140–144	0	41.98	821.70	137.95	83.97	12.00	83.97	587.78	0	18	21700	201	406
108-658A-10H-1, 12–16	0	10.54	400.70	237.25	15.82	0	42.18	590.50	0	15	24200	306	304
108-658A-10H-1, 81–85	0	0	529.74	446.76	38.29	6.38	159.56	982.88	12.76	17	21700	200	398
108-658A-10H-2, 12–16	0	7.56	695.75	476.44	98.31	7.56	90.75	589.87	0	16	24200	200	316
108-658A-10H-2, 81–85	0	57.44	2118.94	631.85	229.76	19.15	57.44	772.26	0	17	21700	200	820
108-658A-10H-3, 12–16	0	49.82	1793.65	427.06	291.82	14.24	78.29	341.65	0	17	24200	200	528
108-658A-10H-3, 81–85	0	6.38	982.88	1085.00	82.97	0	70.21	931.82	0	17	21700	200	591
108-658A-10H-4, 12–16	0	96.80	2976.60	572.73	80.67	8.07	80.67	766.33	0	15	24200	200	773
108-658A-10H-4, 81–85	0	6.03	789.64	96.44	223.03	6.03	72.33	283.31	0	18	21700	200	340
108-658A-10H-5, 12–16	0	0	646.46	78.70	44.97	11.24	140.53	286.69	0	15	24200	287	306
108-658A-10H-5, 84–88	0	44.68	1167.97	319.12	44.68	25.53	102.12	376.56	0	17	21700	200	471
108-658A-10H-6, 12–16	0	0	226.93	283.66	12.16	0	93.20	506.54	8.10	17	21700	315	312
108-658A-10H-6, 65–69	0	40.69	596.75	406.88	20.34	0	108.50	705.25	0	16	21700	200	329
108-658A-11H-2, 12–16	0	5.51	330.79	281.17	16.54	0	154.37	611.97	0	16	21700	246	309
108-658A-11H-3, 12–16	0	7.23	622.07	585.90	28.93	0	72.33	752.27	0	15	21700	200	341
108-658A-11H-4, 12–16	0	6.78	1078.22	223.78	27.13	6.78	176.31	420.44	13.56	16	21700	200	385
108-658A-11H-5, 12–16	0	0	1755.15	63.82	25.53	12.76	38.29	408.47	0	17	21700	200	537
108-658A-11H-6, 12–16	0	0	746.74	102.12	153.18	6.38	76.59	427.62	0	17	21700	200	328
108-658A-11H-7, 12–16	16.81	0	2218.33	285.69	50.42	0	134.44	974.72	0	15	12100	48	301
108-658A-11H-8, 12–16	0	19.15	555.26	536.12	108.50	0	70.21	1250.94	19.15	17	21700	200	465
108-658A-12H-1, 12–16	0	28.93	1222.43	1381.57	57.87	0	65.10	2155.53	7.23	15	21700	200	794
108-658A-12H-2, 12–16	0	21.70	2177.23	1504.53	347.20	14.47	36.17	1171.80	7.23	15	21700	200	889

Note: Pollen concentration values are given in number (*n*) per cm<sup>3</sup>. *Lycopodium* was used as a marker spore. The influx values mentioned in this paper are derived by multiplication of the concentration values with the sedimentation rates.